PALAIOS
Emphasizing the impact of life on Earth's history

PALAIOS, 2022, v. 00, 1–26
Research Article
DOI: http://dx.doi.org/10.2110/palo.2021.051

END-PERMIAN BURNOUT: THE ROLE OF PERMIAN–TRIASSIC WILDFIRES IN EXTINCTION, CARBON CYCLING, AND ENVIRONMENTAL CHANGE IN EASTERN GONDWANA

CHRIS MAYS[1] AND STEPHEN MCLOUGHLIN[2]
[1]School of Biological, Earth and Environmental Sciences, Environmental Research Institute, University College Cork, Distillery Fields, Cork T23 N73K, Ireland
[2]Swedish Museum of Natural History, Svante Arrhenius v. 9, SE-104 05, Stockholm, Sweden
email: cmays@ucc.ie

ABSTRACT: **Wildfire has been implicated as a potential driver of deforestation and continental biodiversity loss during the end-Permian extinction event (EPE; ~ 252 Ma). However, it cannot be established whether wildfire activity was anomalous during the EPE without valid pre- and post-EPE baselines. Here, we assess the changes in wildfire activity in the high-latitude lowlands of eastern Gondwana by presenting new long-term, quantitative late Permian (Lopingian) to Early Triassic records of dispersed fossil charcoal and inertinite from sediments of the Sydney Basin, eastern Australia. We also document little-transported fossil charcoal occurrences in middle to late Permian (Guadalupian to Lopingian) permineralized peats of the Lambert Graben, East Antarctica, and Sydney and Bowen basins, eastern Australia, indicating that even vegetation of consistently moist high-latitude settings was prone to regular fire events. Our records show that wildfires were consistently prevalent through the Lopingian, but the EPE demonstrates a clear spike in activity. The relatively low charcoal and inertinite baseline for the Early Triassic is likely due in part to the lower vegetation density, which would have limited fire spread. We review the evidence for middle Permian to Lower Triassic charcoal in the geosphere, and the impacts of wildfires on sedimentation processes and the evolution of landscapes. Moreover, we assess the evidence of continental extinction drivers during the EPE within eastern Australia, and critically evaluate the role of wildfires as a cause and consequence of ecosystem collapse. The initial intensification of the fire regime during the EPE likely played a role in the initial loss of wetland carbon sinks, and contributed to increased greenhouse gas emissions and land and freshwater ecosystem changes. However, we conclude that elevated wildfire frequency was a short-lived phenomenon; recurrent wildfire events were unlikely to be the direct cause of the subsequent long-term absence of peat-forming wetland vegetation, and the associated 'coal gap' of the Early Triassic.**

INTRODUCTION

Changes in modern fire regimes are providing unequivocal stress on modern land ecosystems (Kelly et al. 2020). The impacts of wildfire have been starkly illustrated by recent mass-killings of terrestrial animals and plants (e.g., southeastern Australia, 2019–2020: Ward et al. 2020; Gallagher et al. 2021; Geary et al. 2021) and unprecedented habitat loss (e.g., Pantanal, South America, 2019–2021: Feng et al. 2021; Pivello et al. 2021). The climatic conditions that lead to such wildfire events are likely to increase (Seneviratne et al. 2021). For example, the fire-prone climatic and ecological conditions that promoted the southeast Australian megafires (e.g., elevated air temperature maxima, low summer precipitation, and regenerative success of fire-adapted plant taxa) are projected to be four times more prevalent within the next 50 years (van Oldenborgh et al. 2021). In light of these recent findings, the potential for wildfires as a direct extinction driver during hyperthermal events, rather than an epiphenomenon of climatic changes (e.g., aridification, warming), deserves further examination.

The end-Permian extinction event (c. 252 million years ago; Burgess et al. 2014; Fielding et al. 2019) was the most severe mass extinction in Earth's history. This hyperthermal event has been linked to the extinction of $\geq$ 80% of ocean animal species (Stanley 2016) and the collapse of land (Benton and Newell 2014; Feng et al. 2020a; Biswas et al. 2020) and freshwater (Mays et al. 2021b) ecosystems. This event resulted in the abrupt extirpation of the primary coal-forming carbon sinks, such as the *Glossopteris* biome of Gondwana (Mays et al. 2020; Vajda et al. 2020) and the tropical gigantopterid and conifer forests of east Asia (Chu et al. 2020). Evidence is converging on the Siberian Traps Large Igneous Province (Siberian Traps herein), a vast region of magmatic emplacement and volcanic eruption in northern Eurasia, as the ultimate cause of this extinction event (e.g., Reichow et al. 2009; Sobolev et al. 2011; Burgess et al. 2017). As a result of the Siberian Traps, a series of plausible direct kill mechanisms, or 'extinction drivers', have been proposed for the loss of marine species (see review by Dal Corso et al. 2022). However, owing to a relative paucity of continental successions with precise age-constraints, the drivers of continental extinctions have received less attention.

Several Siberian Traps-related extinction drivers have been advanced for continental ecological collapse during the EPE, including severe temperature increase (Bernardi et al. 2018; Frank et al. 2021), freshwater microbial blooms (Mays et al. 2021a), acid rain (Black et al. 2014; Sephton et al. 2015), heavy metal toxicity (see review by Grasby et al. 2020) and ozone depletion leading to enhanced UV-B radiation (Visscher et al. 2004; Beerling et al. 2007; Black et al. 2014; Benca et al. 2018). Wildfire, the combustion of land vegetation, has also been advanced as a potential EPE extinction driver on land (Feng et al. 2020b; Cai et al. 2021b), supported by an increase in fossil charcoal (Shen et al. 2011b; Zhang et al. 2016; Chu et al. 2020; Cai et al. 2021a, 2021b), soot (Shen et al. 2011a), and polycyclic aromatic hydrocarbons (PAHs; Grice et al. 2007; Nabbefeld et al. 2010; Shen et al. 2011b; Zhou et al. 2021; see review by Baker 2022). However,

Published Online: Month 2022
 0883-1351/22/000-000

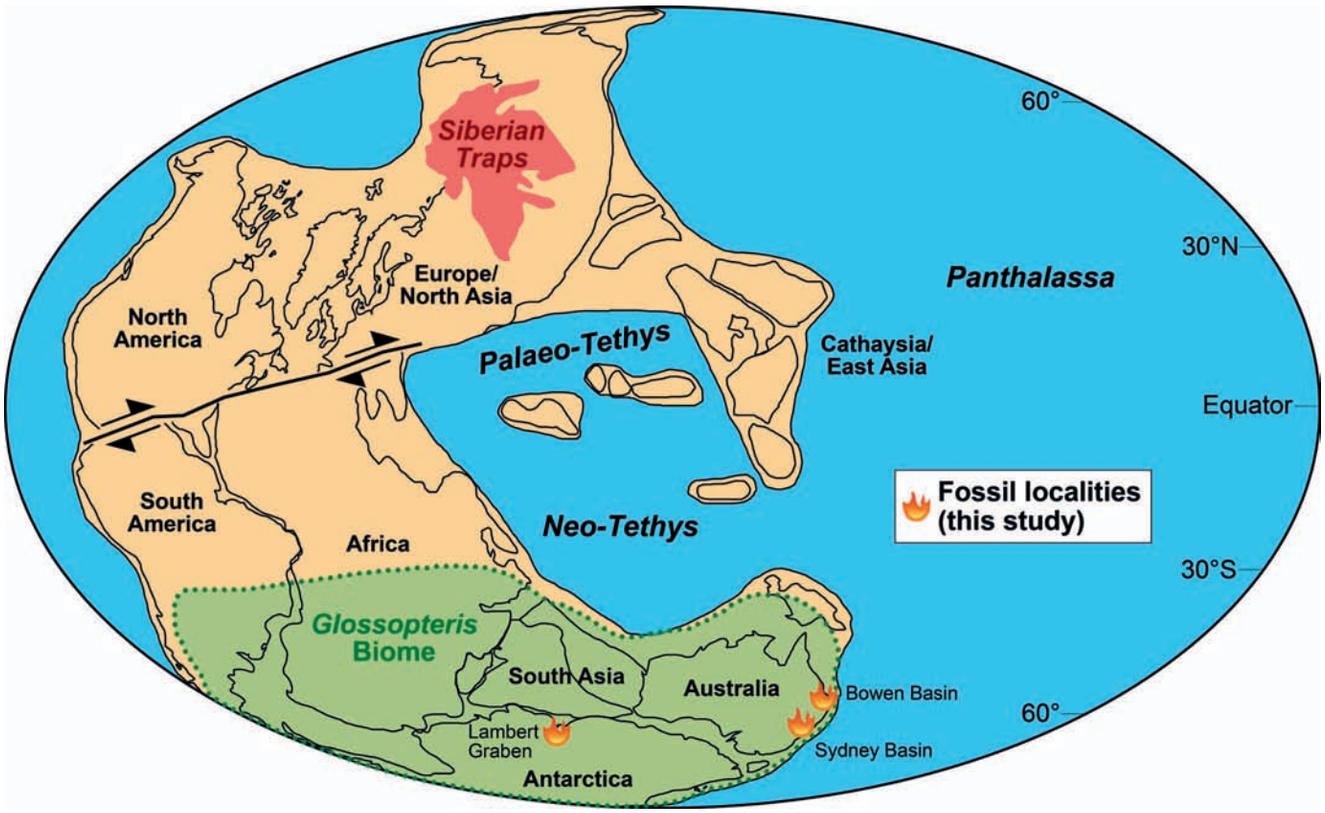

FIG. 1.—Permian–Triassic paleogeography (~ 250 Ma), map adapted from Muttoni et al. (2009), distributions of *Glossopteris* biome and Siberian Traps Large Igneous Province from McLoughlin (2001) and Reichow et al. (2009), respectively.

wildfires were frequent and widespread throughout the late Permian (Lopingian Epoch; 259.51–251.9 Ma), the interval leading up to the EPE, without any accompanying major biodiversity loss or discernible ecosystem disruption. Evidence for global fire-prone conditions during the Lopingian has grown steadily in the last 20 years, such as abundant macroscopic charcoal (or macro-charcoal) in Antarctica (Tewari et al. 2015), Australia (Glasspool 2000; McLoughlin et al. 2019), Europe (Uhl and Kerp 2003; Uhl et al. 2012; Kustatscher et al. 2017), Brazil (Kauffmann et al. 2016), China (Yan et al. 2019; Xiao et al. 2020), Jordan (Uhl et al. 2007), and south Asia (Jasper et al. 2012, 2016a, 2016b; Mahesh et al. 2015; Shivanna et al. 2017). Similarly, abundance trends of 'inertinite' (see Materials and Methods) have indicated significant fluctuations in wildfire activity during the Lopingian, but upon a background of relatively high fire activity (Diessel 2010; Glasspool and Scott 2010; Glasspool et al. 2015). Hence, for wildfires to serve as a causative agent for continental extinctions during the EPE, their prevalence would need to have reached extreme levels above an already high Lopingian baseline.

When assessing deep-time paleowildfires, dispersed fossil charcoal ('fusinite' and 'semi-fusinite') is typically considered the most diagnostic form of evidence (Scott and Glasspool 2007; Scott 2010). Fossil soot can be derived from the combustion of hydrocarbons rather than vegetation (Kaiho et al. 2016), while combustion-related PAHs can have various sources (Whiteside and Grice 2016; Kaiho et al. 2021). By studying fossil charcoal and plant records, the present study aims to critically evaluate the prevalence of fire and evidence of fire adaptations in the pre-EPE Permian wetlands of eastern Australia. Moreover, we aim to provide long-term wildfire trends for the late Permian and Early Triassic to establish whether the EPE was an interval of anomalous wildfire prevalence. Finally, we aim to fill a conspicuous global gap in the evidence for post-EPE wildfires, and test whether wildfire activity persisted, at least regionally, during the Early Triassic.

GEOLOGICAL SETTING

The Sydney Basin was largely situated within or near the south polar circle (~ 60–70°S: Veevers 2006; or ~ 80–90°S: Klootwijk 2016) during the late Permian and Early Triassic (Fig. 1). The basin forms part of an extensive continental foreland basin complex, bounded on its eastern side by a subduction-related volcanic arc, the New England Orogen, which was active from the Late Carboniferous until at least the Middle Triassic (Waschbusch et al. 2009). Microscopic inertinite (~ micro-charcoal; see Materials and Methods) counts were collected from strata of the upper Illawarra Coal Measures (and coeval upper Newcastle Coal Measures) and the overlying Narrabeen Group. These units were deposited within alluvial, deltaic, lacustrine and/or mire settings on vast coastal/alluvial plain systems (Fielding et al. 2021). Recent radiogenic isotope data have constrained the age of the target strata to the Changhsingian–Olenekian ages (late Lopingian–late Early Triassic, ~ 253–248 Ma; Metcalfe et al. 2015; Fielding et al. 2019, 2021). Sedimentary successions in the five target sections (Fig. 2B) have been correlated to the regional spore-pollen biostratigraphic scheme originally defined by Foster (1982), and later correlated to the global chronostratigraphy (Mays et al. 2020). The spore-pollen biozones can be categorized into two broad temporal intervals: the pre-EPE (*Dulhuntyispora parvithola* Zone) and the post-EPE (in ascending order: *Playfordiaspora crenulata* Zone, *Protohaploxypinus microcorpus* Zone, *Lunatisporites pellucidus* Zone, *Protohaploxypinus samoilovichii* Zone, and *Aratrisporites tenuispinosus* Zone; Fig. 3).

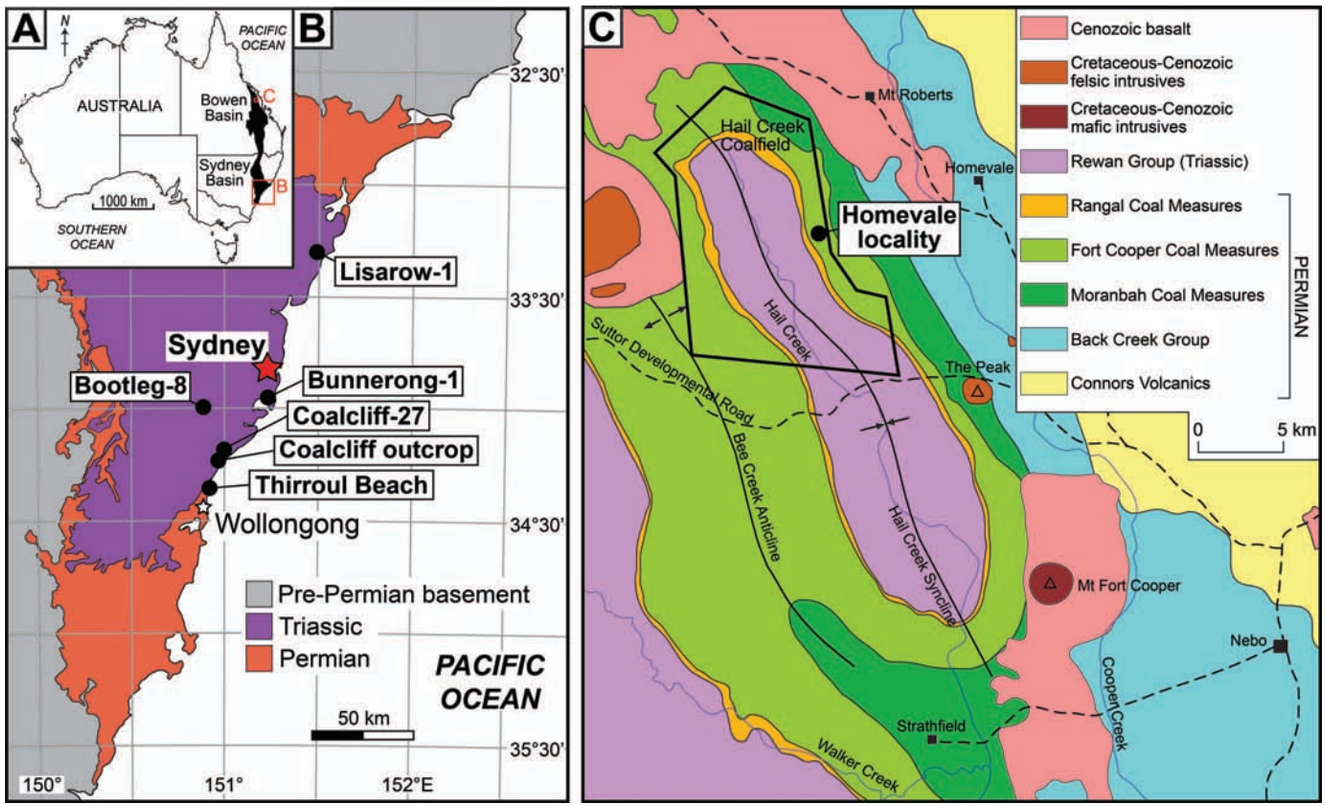

FIG. 2.—Geological maps of eastern Australian fossil localities. **A**) Map of Australia. **B**) Simplified geological map of the Sydney Basin, with distributions of Permian and Triassic strata; updated from Fielding et al. (2019). **C**) Geological map of the Homevale Locality, northern Bowen Basin, adapted from McLoughlin et al. (2018).

The continental end-Permian extinction horizon (EPE; ~ 252.2 Ma) has been correlated across the basin and is concurrent with the upper surface of the uppermost coal bed of the Illawarra/Newcastle Coal Measures (Fielding et al. 2019; McLoughlin et al. 2021; Fig. 3). The EPE corresponds to the contact between the *D. parvithola* and *P. crenulata* zones (Mays et al. 2020); however, an informal biostratigraphic 'dead zone' (*sensu* Vajda et al. 2020), characterized by an absence of identifiable fossil index taxa, has been identified in a thin interval immediately above the upper *D. parvithola* Zone boundary (= EPE), and is more or less correlative with the Frazer Beach Member (uppermost Illawarra/Newcastle Coal Measures; McLoughlin et al. 2021). The EPE also marks the last undisputed occurrence of glossopterid macrofloral remains (e.g., *Glossopteris*, *Plumsteadia*, *Vertebraria*; McLoughlin et al. 2021).

The pre-EPE Lopingian fossil floras of the Sydney Basin are typical of the glossopterid biome (Fig. 1), a widespread, low-diversity, forest-mire vegetation (Mays et al. 2020) that developed in cool-temperate, high-precipitation conditions (Frank et al. 2021). Today, these mire deposits are represented by thick bituminous coal seams, or less commonly, siliceous permineralized peats (Pigg and McLoughlin 1997; McLoughlin et al. 2019). At the onset of the EPE, the basin experienced an increase in temperature (≥ 10°C; Frank et al. 2021) and enhanced precipitation seasonality (Fielding et al. 2019). Immediately following the EPE (equivalent to the 'dead zone'; lower Frazer Beach Member), the lowlands experienced an interval of ponding, owing to the rapid deforestation of the glossopterid biome, subsequent decrease in evapotranspiration, and elevation of water tables (Vajda et al. 2020). From the post-EPE Lopingian (c. 252.2 Ma) until the Spathian (late Early Triassic; ~ 249 Ma), the region hosted a sparse vegetation dominated by sclerophyllous corystosperms, peltasperms and conifers, with an understory of ferns and pleuromeian lycophytes (Retallack 1980; Mays et al. 2020). A persistently hot and seasonally dry climate (Frank et al. 2021) precluded the formation of peat-forming conditions from eastern Australia in the Early Triassic (Retallack et al. 1996). Instead, the Sydney Basin experienced intermittent inundation of the floodbasins, forming lakes inhabited by thriving chlorophyte algal and bacterial communities (Mays et al. 2021a).

In addition to evaluating meso- and micro-charcoal abundance from bore-core samples, we also investigated macro- and meso-charcoal within three deposits of Guadalupian to Lopingian permineralized peats from eastern Gondwana to provide benchmarks for typical charcoal abundance and associations in pre-EPE high-latitude, peat-forming ecosystems. Vertical sections cut through permineralized blocks yielded profiles through the relatively uncompressed detritus that made up the original peat column and provide information on the spatial distribution of autochthonous and allochthonous plant components, the abundance of charcoal, and the types of plant organs most prone to charcoalification. The permineralized peat samples derive from three deposits: the lower Wilton Formation of the Sydney Basin, southeastern Australia; the Fort Cooper Coal Measures of the northern Bowen Basin, northeastern Australia; and the uppermost bed of the Toploje Member, Lambert Graben, East Antarctica.

A silicified peat block collected from the southern end of Thirroul Beach (34°19′44″S, 150°55′34″E; Fig. 2B) in the southern Sydney Basin derives from the lower Wilton Formation, which was deposited mainly within meandering fluvial channels and associated floodbasin settings (Bamberry 1991; Shi and McLoughlin 1997). McMinn (1985) recognized index taxa of the *Dulhuntyispora parvithola* Zone in the lower part of this unit, denoting a Lopingian age. Radiogenic age constraints of zircons from tuffs in units bracketing the Wilton Formation indicate a Wuchiapingian

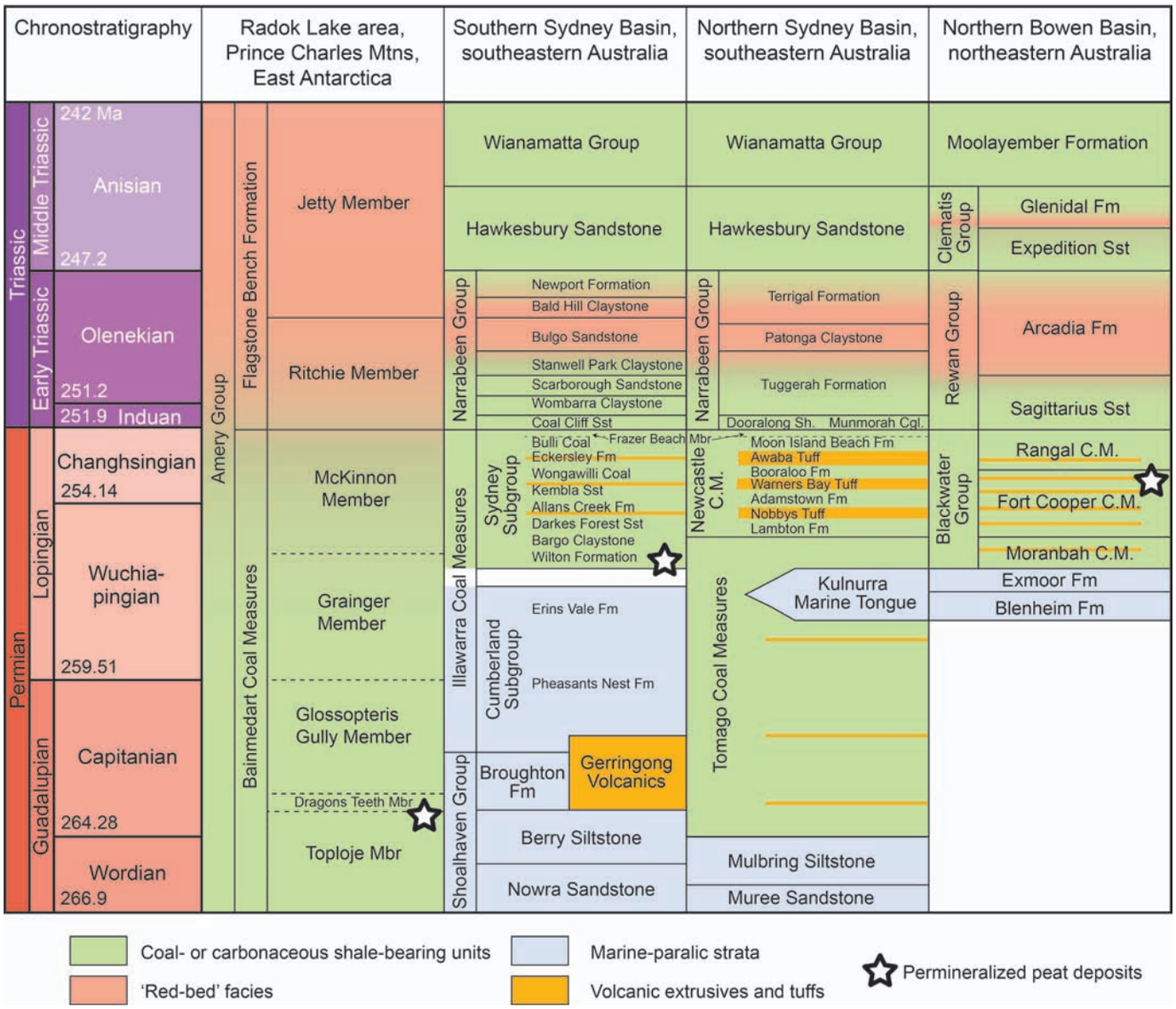

FIG. 3.—Stratigraphic correlation chart for the studied Permian–Triassic successions in the Lambert Graben, East Antarctica and the Sydney and Bowen basins, eastern Australia, showing the distribution of principal depositional settings and the occurrences of permineralized peat studied herein.

(early late Permian) age for this unit (Huyskens 2014; Metcalfe et al. 2015). The fossil flora of the Wilton Formation permineralized peat, described by McLoughlin et al. (2019), is dominated by glossopterid remains.

The Fort Cooper Coal Measures constitute the middle coal-bearing unit of the Lopingian Blackwater Group in the northeastern part of the Bowen Basin, Queensland, Australia (Fig. 2C). The unit is dominated by fine-grained siliciclastic rocks and includes thin coals and abundant tuffs deposited predominantly in floodplain lakes and mires (Goscombe 1975; Hutton et al. 1991). A silicified peat within this unit is exposed as a thin erosion-resistant lens extending laterally over several meters and with a vertical extent of < 1 m located at 21°28′ 16.63″S, 148°25′56.12″E just within the western limit of what is now the Homevale National Park. The tuff-rich interval of the Blackwater Group throughout the Bowen Basin contains a spore-pollen assemblage assigned to the Upper Stage 5b–5c (*Microreticulatispora bitriangularis–Triplexisporites playfordii*) Palynozone of Price (1983) or the APP5 Zone of Price (1997). Chemical Abrasion Isotope Dilution Thermal Ionisation Mass Spectrometry (CA-ID-TIMS) U-Pb dating of zircons from correlative tuffs in the southern Bowen Basin indicate an early Changhsingian age range of 254.10 ± 0.09 Ma to 252.54 ± 0.05 Ma (Laurie et al. 2016). The fossil flora of the Fort Cooper Coal Measures has not been documented in full but studies of specific glossopterid and fern remains have been undertaken by Gould (1970, 1975), Gould and Delevoryas (1977), Pigg and McLoughlin (1997), Nishida et al. (2007, 2013, 2018) and McLoughlin et al. (2018).

The Toploje Member is the lowermost unit of the Bainmedart Coal Measures within the Amery Group (Fig. 4). The unit is exposed only in the Radok Lake area, Prince Charles Mountains, East Antarctica, and incorporates channel and floodbasin deposits of a sandy braided river system. The stratigraphy and sedimentology of the Amery Group, preserved within an intracratonic rift system (Lambert Graben: Harrowfield et al. 2005), were described in detail by Webb and Fielding (1993), Fielding and Webb (1995, 1996) and McLoughlin and Drinnan (1997a, 1997b). Although previously assigned to the Wordian (middle Guadalu-

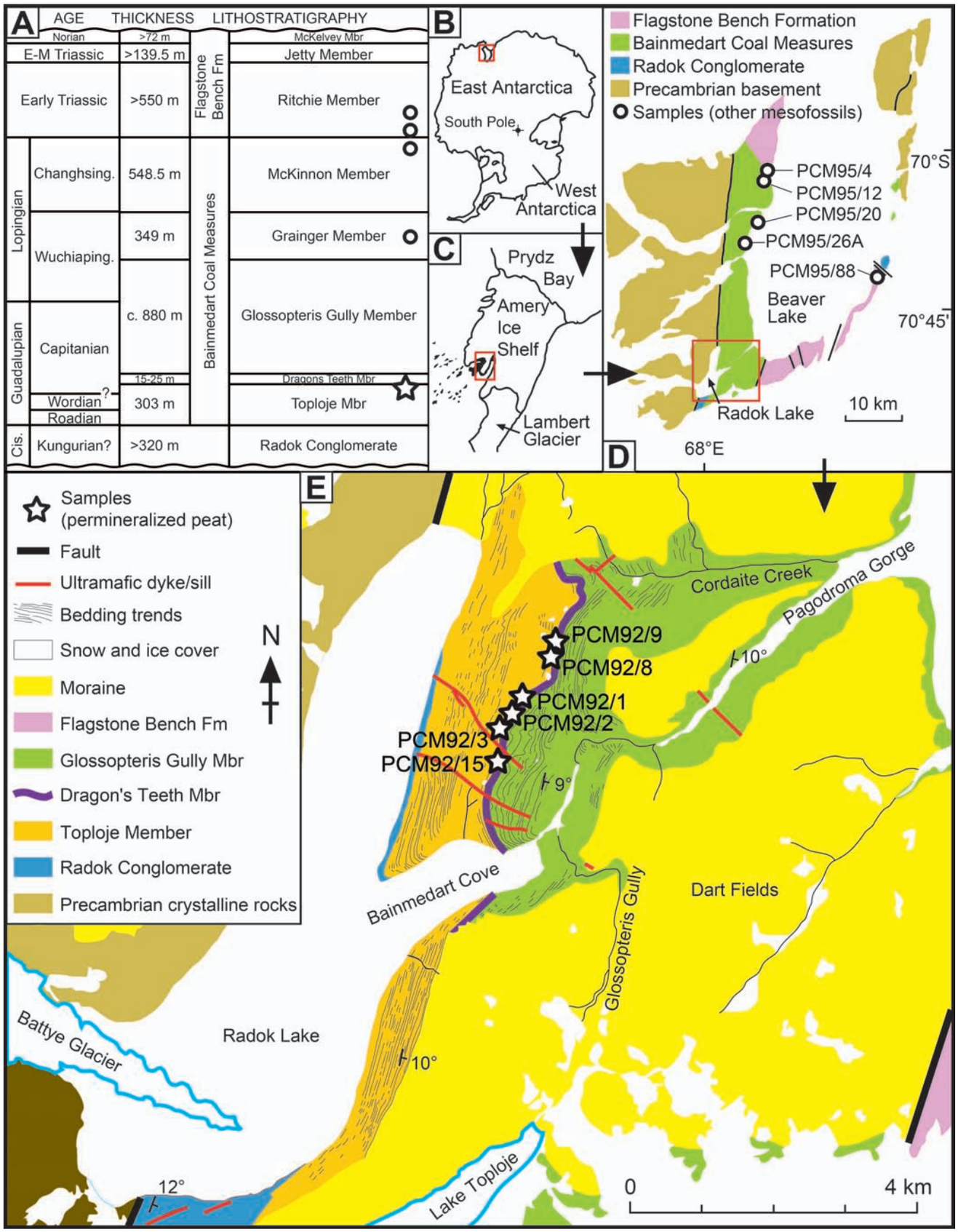

FIG. 4.—Geological maps and lithostratigraphy of the Prince Charles Mountains, East Antarctica; geological maps from McLoughlin and Drinnan (1997a, 1997b), lithostratigraphy from Lindström and McLoughlin (2007). Symbols: stars = permineralized peat localities; circles = other charcoalified fossil localities. **A**) Summary of regional Permian–Triassic lithostratigraphy including stratigraphic placements of samples. Abbreviations: Changhsing. = Changhsingian; Cis. = Cisuralian; Wuchiaping. = Wuchiapingian. **B**) Map of Antarctica. **C**) Map of the Amery Ice Shelf region. **D**) Geological map of the Beaver Lake area. **E**) Geological map of the Radok Lake area.

pian) based on palynological criteria (McLoughlin et al. 1997; Lindström and McLoughlin 2007), recent recalibration of the reference palynozones in eastern Australia by CA-ID-TIMS U-Pb dating of zircons from tuffs suggests that the uppermost bed of the Toploje Member may be as young as mid-Capitanian (late Guadalupian, ~ 262 Ma; Laurie et al. 2016). The Radok Lake area was located at ~ 65–70°S during the Guadalupian (Scotese and Langford 1995; Torsvik et al. 2012; Fig. 1). The plant fossil assemblage from the Toploje Member peat has been documented by Neish et al. (1993), McLoughlin and Drinnan (1996), Weaver et al. (1997), McLoughlin et al. (2015), and Slater et al. (2011, 2012, 2013, 2015). The associated palynoflora has been documented by McLoughlin et al. (1997) and Lindström and McLoughlin (2007).

MATERIAL AND METHODS

Terminology

Following Scott (2010), fossil charcoal was identified by its black color, silky luster, very high reflectivity, general lath-shaped form, and splintery texture. These grains commonly have well-preserved cellular structure with homogenized walls, and a tendency to fracture longitudinally owing to contraction of cell walls away from the middle lamella (Jones and Chaloner 1991). The term 'inertinite' is utilized following the International Committee for Coal and Organic Petrology (ICCP 2001), which circumscribes a microscopic maceral group with high reflectance and, when derived from woody plant remains, typically preserves cellular structures (e.g., the coal macerals 'fusinite' and 'semifusinite'). In bituminous coals and associated sediments, such as those of the Lopingian Sydney Basin (% mean maximum reflectance of vitrinite = 0.6–1.1; Huleatt 1991), inertinite can be differentiated by its higher reflectance than vitrinite (ICCP 2001). Despite some documented cases to the contrary (Hower et al. 2011; Richardson et al. 2012), the pyrogenic nature of almost all inertinite in the geological record has been established by taphonomic experiments (Scott 2000; Scott and Glasspool 2006), geochemical analyses (Moroeng et al. 2018), and modern analogues (Scott et al. 2000). Hence, relative inertinite abundances are employed herein as a proxy for wildfire activity. However, owing to the relatively high thermal maturity of these sediments, some misidentification of vitrinite as inertinite is possible. If so, this would lead to a systematic, but consistent (given the relatively uniform thermal maturity across the basin), overestimation of inertinite abundances. Hence, we employ only the relative (rather than absolute) abundance of inertinite in this study for gauging changes in wildfire prevalence.

Inertinite from Shale and Coal Palynological Preparations

Quantitative plant microfossil and inertinite data were collected from palynological samples recovered from the following five successions spanning the Permian–Triassic transition (Fig. 5): (1) AGL Bootleg DDH 8 bore core (Bootleg-8), central Sydney Basin (33°59′56.62"S, 150°44′13.43"E); (2) Coalcliff outcrop, southern Sydney Basin (34°15′18.90″S, 150°58′22.20″E); (3) Coal Cliff Colliery DDH 27 bore core (Coalcliff-27), southern Sydney Basin (34°13′25.28″S, 150°56′50.67″E); (4) Pacific Power Hawkesbury Bunnerong DDH 1 bore core (Bunnerong-1), central Sydney Basin (33°58′17.61″S, 151°13′43.52″E); and (5) Elecom Hawkesbury Lisarow DDH 1 bore core (Lisarow-1), northern Sydney Basin (33°22′38.54"S, 151°23′0.53"E). In Bunnerong-1 and Coalcliff-27, most of the uppermost Permian coal seam (Bulli Coal) and part of the overlying Frazer Beach Member were removed for geotechnical analysis soon after drilling, so these could not be analyzed herein (Fig. 5B). Samples were processed for organic microfossils at Global Geolab, Medicine Hat, Canada. Inorganic mineral content was removed from sediment samples using hydrochloric (HCl) and hydrofluoric (HF) acids. Resultant organic residues were oxidized with Schulze's Solution, sieved (upper sieve 150 μm, lower sieve 5 μm [Bootleg-8, Lisarow-1] or 10 μm [Coalcliff outcrop, Coalcliff-27, Bunnerong-1]), mounted on glass slides, and glass coverslips were sealed with epoxy.

Transmitted light microscopy and photomicrography of plant microfossils and inertinite specimens were conducted using a Zeiss Axioskop 2 transmitted light microscope with differential interference contrast and equipped with a Canon EOS 700D DSLR camera.

As noted by Batten (1996, p. 1033), identifying charcoalified plant debris with transmitted light microscopy alone is problematic. With this method, we identified rare, semi-transparent tracheid specimens (Fig. 6B, 6C) that exhibited features (e.g., fracturing, wall thinning, cell distortion, discoloration) typical of high temperature burning under experimental conditions (Braadbaart and Poole 2008; Hudspith and Belcher 2017). However, their rarity precluded valid quantification. More commonly, micro-charcoal could not be adequately distinguished under transmitted light from other opaque lath-shaped wood fragments (Highton et al. 1991; Batten 1996; Glasspool and Scott 2013; see Tyson 1995). To circumvent these issues, inertinite counts were conducted using reflected light microscopy (Fig. 6D–6G) using a Nikon SMZ25 stereomicroscope, equipped with a Nikon DS-Fi3 camera. These counts were conducted on the same slides for which quantitative plant microfossil analysis was undertaken. Specimens were illuminated by a pair of orthogonal gooseneck spot lights directed at low angles (5–10°) to the sample stage, powered by a Nikon C-FLED2 LED light source. A total of 146 palynological samples were included: 31 from Bootleg-8, 14 from Coalcliff outcrop, 23 from Coalcliff-27, 50 from Bunnerong-1, and 28 from Lisarow-1. For each sample, all organically preserved grains ('palynofacies' *sensu* Tyson 1995) were counted, with a minimum count of 250 individual 'phytoclasts' (which includes all woody remains of land plants). Phytoclasts were categorized as: (1) inertinite and (2) others. Inertinite abundances are provided separately as proportions of total palynofacies grains (for comparison to other studies, which have generally applied this approach as the standard procedure), and as a proportion of total phytoclasts (Online Supplemental File Table S1). In this study, the latter proportions were considered a more reliable gauge of wildfire prevalence trends (Fig. 5B) than the former, since by examining only the woody remains of plants, this controls for variations in other acid-resistant organic remains. Previous studies have demonstrated that non-wood remains (e.g., algal cells, microbially derived organic matter, spores/pollen) fluctuate significantly throughout continental Permian–Triassic strata of the region (e.g., Vajda et al. 2020; Wheeler et al. 2020; Mays et al. 2021a). Therefore, relative inertinite abundance statistics refer to proportions of phytoclasts, unless otherwise stated.

To increase the internal validity of the inertinite trends and avoid potential observer biases, two successions (Bootleg-8 and Lisarow-1) were counted using the following blind protocol: (1) all slide labels were masked; (2) slide order was randomized; and (3) sample counts were then conducted, as outlined above. Other successions were counted unblinded and in stratigraphic order. To minimize inter-sample depositional biases, only inertinite data collected from fine grained lithofacies (claystone, siltstone, or heterolithic [interbedded silt-/sandstone]) are included in all statistics and Figure 5; all other lithofacies (such as coal, sandstone or tuff) were excluded.

All palynological samples and slides are housed at the Department of Palaeobiology, Swedish Museum of Natural History (Naturhistoriska riksmuseet), Stockholm, Sweden; these are provided with the prefix 'S', and slides are indicated by number suffixes. The sources for the spore-pollen biostratigraphic correlations are as follows: Bootleg-8, Coalcliff outcrop, and Lisarow-1 (Mays et al. 2021a); Bunnerong-1 (Fielding et al. 2019); Coalcliff-27 (Mays et al. 2020). Statistical confidence intervals are equivalent to one standard deviation (s.d.).

For comparison of the present inertinite data to the regional trend, previously published inertinite records from eastern Australia were compiled (Online Supplemental File Table S2). Radiogenic age controls in this region have permitted the correlation of these deposits to the calibrated chronostratigraphy of eastern Australia, and placement into ~ 100 kyrs time

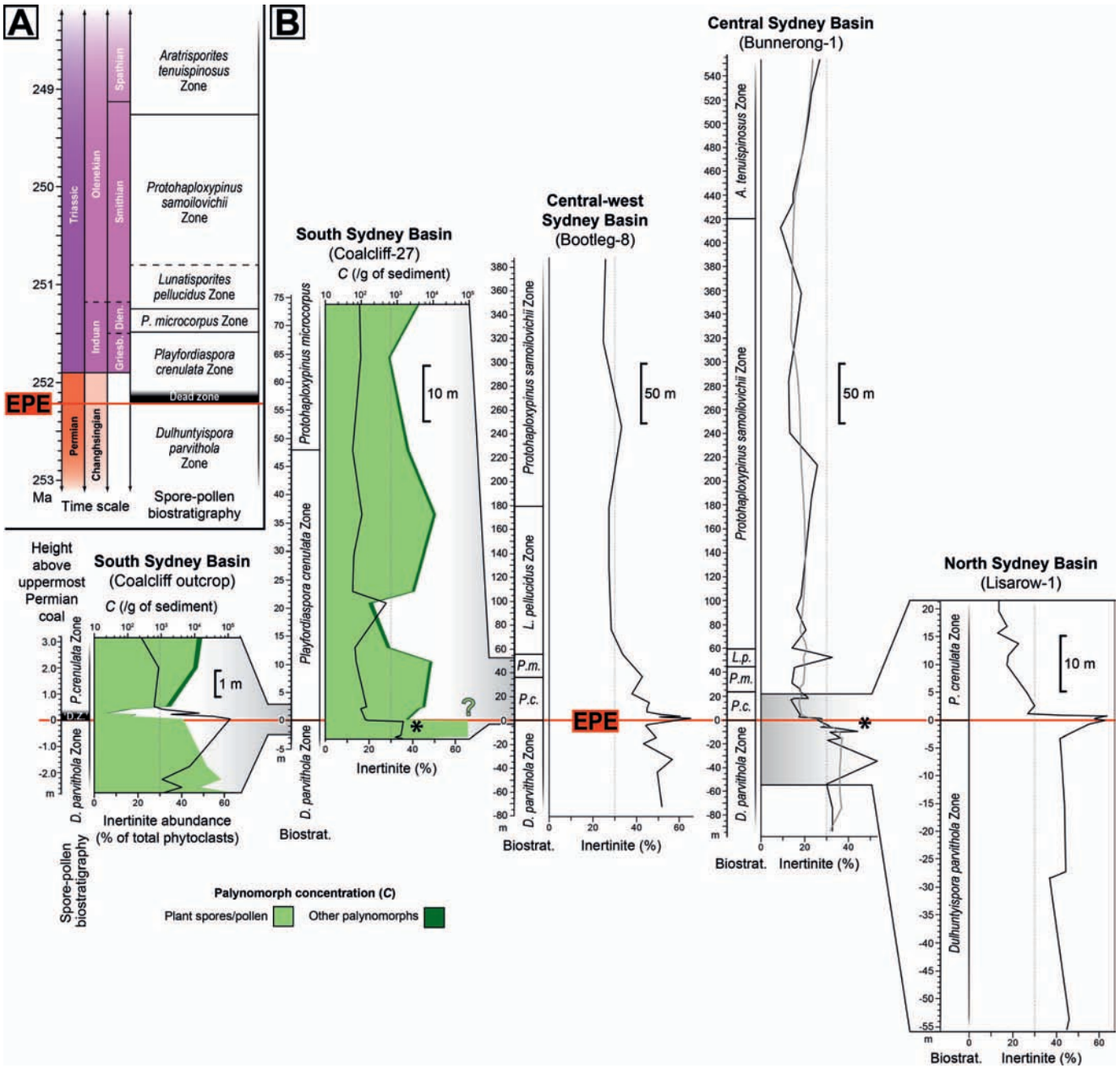

FIG. 5.—Inertinite abundances, palynomorph concentrations and chronostratigraphy of the Sydney Basin, Australia; the continental end-Permian extinction event (EPE) is equivalent to the top of the uppermost Permian coal beds. **A**) Biostratigraphy of the Sydney Basin correlated to the global chronostratigraphy. Abbreviations: Dien. = Dienerian; Griesb. = Griesbachian. **B**) Inertinite records of the Sydney Basin, as a proportion (%) of total phytoclasts; dotted line at 30% inertinite abundance for ease of comparison between successions. Key: gray line (Bunnerong-1 only) = 5-point average abundance; ? = concentration estimates exceeded the maximum; * = continuous records for the uppermost Illawarra Coal Measures were unavailable from these successions; *P. microcorpus* Zone = *Protohaploxypinus microcorpus* Zone. Palynomorph concentrations (*C*) from Mays et al. (2020, 2021a).

bins. Age calibration sources: Huyskens (2014), Metcalfe et al. (2015), Ayaz et al. (2016a), Laurie et al. (2016), Phillips et al. (2018), Fielding et al. (2019, 2021), Mays et al. (2020), and Todd et al. (2021).

Charcoal from Permineralized Peat

Samples of silicified peat from all three permineralized plant assemblages outlined above were cut with a diamond saw, polished with a lapidary wheel using 600 grade carborundum powder, and sectioned using the acetate peel technique employing 50-µm-thick cellulose acetate sheets (Hass and Rowe 1999), and standard petrographic thin-sectioning protocols to thicknesses of 50 µm in order to obtain optimal clarity of cell structures (Galtier and Phillips 1999). Portions of acetate peels were cut and mounted on glass slides under a coverslip in Histomount (National Diagnostics). Photomicrographs were taken with an Olympus BX-51 compound transmitted light microscope and an Olympus SZX10

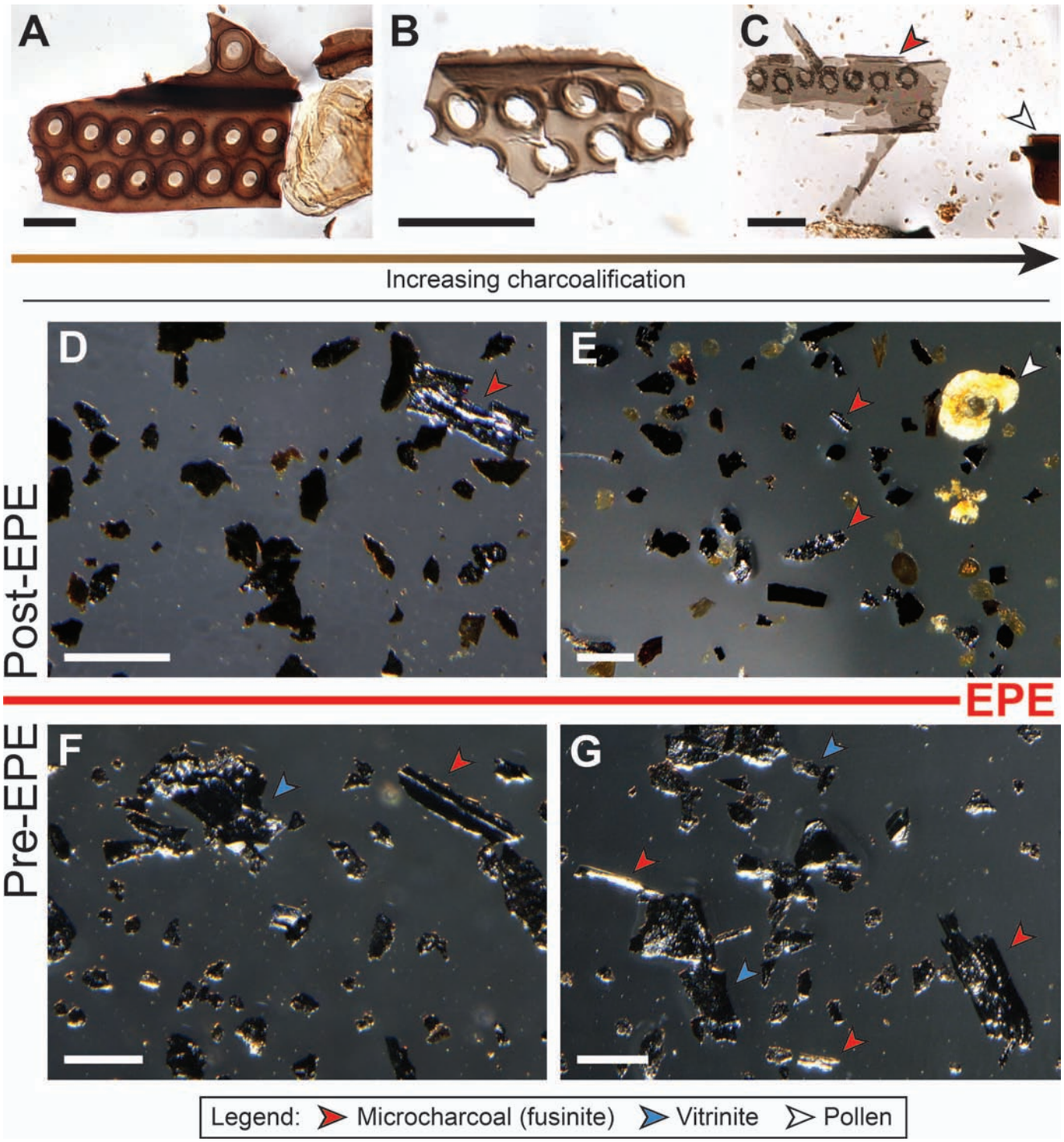

FIG. 6.—Light microscopy images of microscopic plant fossils from the Sydney Basin, Australia; EPE = continental end-Permian extinction event. **A**–**C**) Transmitted light photomicrographs of gymnosperm (?glossopterid) tracheids with differing degrees of charcoalification, all specimens from one pre-EPE shale sample (Loddon Sandstone, Coalcliff outcrop, 220–230 cm below the EPE horizon, S029702), all scales = 20 μm: **A**) well-preserved tracheid with biseriate, oval bordered pits. **B**) Partially charcoalified tracheid, note: discolouration and fractured pit borders. **C**) Tracheid with high degree of charcoalification, note: the high friability and absence of color compared to an unburned tracheid (white arrow); such specimens were very rarely observed under light microscopy. **D**–**G**) Reflected light photomicrographs of palynological assemblages, all scales = 100 μm: **D**) Post-EPE assemblage, note: the scarcity of highly reflective macerals, e.g., inertinite (Coalcliff-27, 470.30 m, S014161). **E**) Post-EPE assemblage (Bunnerong-1, 778.57 m, S014114). **F**) Pre-EPE assemblage, note that the vitrinite exhibits conchoidal fracture with no discernible anatomical details, while inertinite is distinctly lath-shaped (Coalcliff outcrop, 270–280 cm below the EPE horizon, S029700). **G**) Pre-EPE assemblage (Coalcliff outcrop, 170–180 cm below the EPE horizon, S029703).

stereomicroscope, each equipped with an Olympus DP-71 digital camera. Quantitative analysis was undertaken by point-counting at increments of 200 μm along transects across 20 thin sections cut perpendicular to peat bedding for both the Radok Lake and Homevale peats (total of 4000 points each), and 14 thin sections (total of 1753 data points) for the thinner Thirroul Beach peat. Compositional proportions from point counts include void spaces (Online Supplemental File Table S3).

Several samples of permineralized peat were selected for bulk maceration to isolate mesoscopic (0.18–5 mm) charcoalified plant remains ('meso-charcoal') for scanning electron microscopy. These samples were broken into ~ 2 cm^3 blocks, immersed in cold 48% hydrofluoric acid for two weeks to remove the silica, after which the coarse organic debris was recovered using a 180 μm nylon sieve. Sieved organic remains were placed into a petri dish of distilled water, studied with an optical stereomicroscope and charcoalified remains were picked using a camel-hair brush, mounted on aluminium stubs, sputter-coated with gold, and imaged with a Philips FEI Quanta Field Emission Gun 650 scanning electron microscope at the Swedish Museum of Natural History.

Permineralized peat and mesofossil samples are housed at the Swedish Museum of Natural History (Stockholm) with the registration prefix S, the Australian Museum (Sydney) with the registration prefix AMF, Museums Victoria (Melbourne) with the registration prefix NMVP, and Geoscience Australia (Canberra) with the registration prefix CPC. Portions of individual permineralized peat blocks are labeled with separate lowercase letter suffixes, and the thin sections, cellulose acetate peels, or SEM stubs mounted with mesofossils from these portions are labeled with an additional numerical suffix.

Mesofossils from Shales

Most techniques for the quantitative analysis of mesofossils are adapted from the field of archeobotany but no single approach represents an error-free methodology (Batten 1998; Figueiral and Willcox 1999), not least because some delicate plant remains (e.g., thin cuticles, filamentous trichomes, and fibrous wood) have a propensity to fragment during sample preparation. For the purposes of this study, we were only interested in: (1) the proportion of charcoal particles to other organic remains (dispersed cuticle, seeds, sporangia, leaf fragments, non-charred wood, coal particles) in the size fraction 0.18–5 mm, and (2) the variation in charcoal abundance between samples. For this purpose, samples consisting of 30 g of shale were selected from 43 levels in the Pacific Power Hawkesbury Bunnerong DDH 1 bore core (Bunnerong-1), central Sydney Basin, and processed for organic mesofossils in the same manner as for the bulk dissolution of permineralized peats. The organic residues from each sample were transferred to a petri dish and scanned for charcoalified remains using an Olympus SZX10 stereomicroscope. Yields of mesofossils were highly variable (ranging from negligible to many thousands of organic grains), so quantitative data is based on counts of 300 particles and represented as percentages.

RESULTS

Inertinite and Spore-Pollen Records from Palynological Samples

In all examined successions, pre-EPE assemblages generally have higher relative abundances of inertinite compared to those of the post-EPE interval (Fig. 6D–6G). Pre-EPE mean relative abundances were between 34 ± 1.1% (Coalcliff-27) and 49 ± 4.8% (Bootleg-8; Fig. 5B). The siltstone-hosted inertinite assemblages revealed abundance peaks just above the EPE horizon in three successions: Bootleg-8 (+1.8 m: 65.2%), Coalcliff outcrop (+0 to 10 cm: 62.4%), and Lisarow-1 (+1.43 m: 63.4%). These inertinite peaks were all from samples of the Frazer Beach Member. In the two successions where this peak was absent (Bunnerong-1, Coalcliff-27), part or all of the Frazer Beach Member was unavailable for analysis (see methods and materials), precluding meaningful comparisons. The two coal samples of the Bulli Coal (the uppermost Permian coal seam of the southern Sydney Basin) from Coalcliff outcrop also revealed high inertinite abundances: 63.1% and 64.5% from -80 to -70 cm and -30 to -20 cm, respectively.

Stratigraphically above these inertinite peaks (or the EPE, where no peak was identified), each succession reveals a reduction in mean relative abundance to below their respective pre-EPE values; post-peak (or post-EPE) means: 38.5 ± 9.9% (Bootleg-8), 19.3 ± 5.2% (Bunnerong-1), 16.7 ± 4.2% (Coalcliff-27), and 23.7 ± 8.3% (Lisarow-1). The only exception was the Coalcliff outcrop; owing to the short stratigraphic interval that this outcrop represents, valid long-term pre- and post-EPE comparisons could not be made. Severe post-EPE reductions in spore-pollen concentrations were observed at the Coalcliff outcrop and Coalcliff-27 (Fig. 5).

To gauge the long-term Early Triassic baseline of inertinite abundance in the Sydney Basin, the post-*Playfordiaspora crenulata* Zone assemblages of the three longest successions were examined. These showed relatively low inertinite abundances: 30.6 ± 6.0% (Bootleg-8), 18.6 ± 5.4% (Bunnerong-1), and 14.8 ± 2.1% (Coalcliff-27). These abundances correspond to relative reductions of 37%, 48%, and 56% from pre-EPE baselines, respectively.

Charcoal in Permian Permineralized Peats

Each of the three studied permineralized peats contains the remains of a relatively low diversity macroflora that includes various organs of glossopterid gymnosperms, cordaitaleans, ferns, diminutive heterosporous lycopsids, together with fossils of algae, fungi, oomycetes, and arthropod exoskeletons and coprolites. The Fort Cooper Coal Measures peat has undergone notably more compression (~ 30% pore volume loss) before silicification compared to the < 10% volume loss of the other studied permineralized peats.

Quantitative analysis via point counts of vertical sections reveals that each peat assemblage is overwhelming dominated by glossopterid remains, especially leaves (~ 17–31.8%) and (non-charcoalified) wood (~ 6.8–29%). Compositional differences between the three assemblages are modest (Fig. 7) and relate to both the representation of minor floristic elements and taphonomic features.

The Radok Lake (Toploje Member) peat assemblage is differentiated by the notable proportion of *Noeggerathiopsis* (cordaitalean) leaves (~ 6.8%; Fig. 8F) and *Vertebraria* (glossopterid) roots (~ 28%; Fig. 8C), the presence of lycopsids (~ 0.6%; Figs. 8H, 9N), and the higher proportion of fungi (~ 2.2%) and coprolites (~ 2.8%; Fig. 8I). The Radok Lake assemblage represents a relatively uncompressed, root-dominated peat with a high representation of saprotrophic and detritivorous microbiota. It is representative of a floodbasin peat developed in a continent-interior rift setting dominated by braided fluvial systems.

The Thirroul (Wilton Formation) assemblage has a high representation of glossopterid leaves (almost 30%), contains numerous seeds (~ 7%; Fig. 9A, 9B) and fern leaves (~ 7.6%), few (< 1%) roots, and has a high proportion of indeterminate finely macerated plant detritus (~ 25%). This peat is predominantly composed of subaerial components (leaves and seeds) of mostly deciduous plants. This leaf-mat peat accumulated in coastal plain settings of the Sydney (foreland) Basin.

The Homevale (Fort Cooper Coal Measures) assemblage has high proportions of glossopterid leaves (~ 31%) and wood (~ 29%). This peat is especially notable for its abundant (~ 13%) seeds (Fig. 9I), a more compressed texture (and consequent reduced original pore space), and the presence of numerous silica-filled fractures (Fig. 9E, 9I) that likely derive from post-Permian tectonic activity. This peat is also depauperate in roots and primarily represents an accumulation of shed leaves, twigs and seeds.

The proportion of charcoalified remains (of all plant types) is relatively consistent between the three assemblages (~ 4.5–7%). However, it should

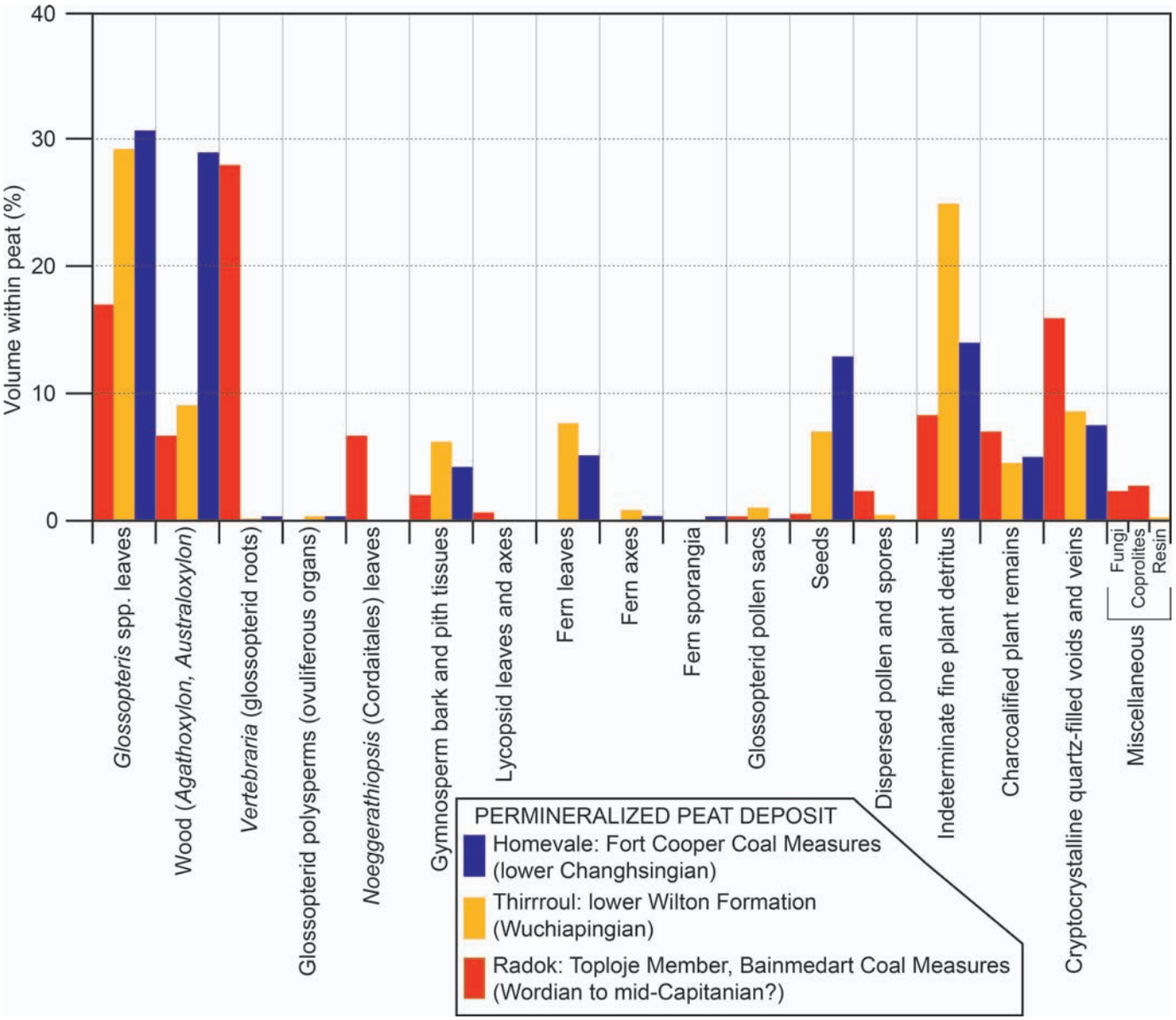

FIG. 7.—Graph of the major components of siliceous permineralized peats from: the Radok Lake area, Prince Charles Mountains, East Antarctica (Toploje Member, Bainmedart Coal Measures: Wordian to mid-Capitanian); Thirroul Beach, southern Sydney Basin, New South Wales, Australia (lower Wilton Formation: Wuchiapingian); and Homevale, northern Bowen Basin, Queensland, Australia (lower Changhsingian).

be noted that these values represent the total plant assemblage. In each deposit, certain peat microfacies are enriched in charcoal to levels of ~ 50% (Slater et al. 2015; McLoughlin et al. 2019). Moreover, charcoalified plant components suffered notably less compression than other plant remains (Fig. 9C, 9E, 9H). Hence, the volumetric representation of charcoal in the strongly compressed Homevale peat probably represents an overestimate compared to the less-compressed Radok Lake and Thirroul Beach peats.

Charcoalified material in all of the peat assemblages is dominated by woody remains (Figs. 7, 8K–8M, 9L). However, bulk dissolution of peat and associated shale samples in hydrofluoric acid also yields charcoalified remains of very delicate plant components including leaves with fine hairs and epidermal details (Fig. 8A, 8B, 8D–8F, 8N–8P), seeds (Fig. 8J, 8R), pollen sacs (Fig. 8G, 8T), and even coprolites (Figs. 8I, 9M). Retention of such delicate cellular details is generally indicative of combustion in low-intensity wildfires with temperatures in the range of 240–370°C (Scott and Jones 1991; McParland et al. 2007). In addition, homogenization of cell walls (Fig. 8R), *en echelon* and brittle conchoidal fracturing (Fig. 8S, 5U), local blistering (Fig. 8Q), and cracking along the middle lamella to segregate cells (Fig. 8T) are all features that develop within experimental charring of woods at temperatures of 230–400°C (Jones and Chaloner 1991). All of the permineralized peats contain macro-charcoal, both as isolated clasts and as rich concentrations along certain laminae (Fig. 10D, 10E). Small, isolated charcoal grains (Fig. 9F, 9K) tend to be relatively angular and may represent components blown into the peat deposit and incorporated rapidly in the matrix. Where macro-charcoal occurs in bands, the individual particles are commonly subrounded (Fig. 9B, 9D, 9I), although not in all cases (Fig. 9G). Only rare examples of allochthonous woody axes show gradation from charred outer surfaces to non-charred interiors (Fig. 9J).

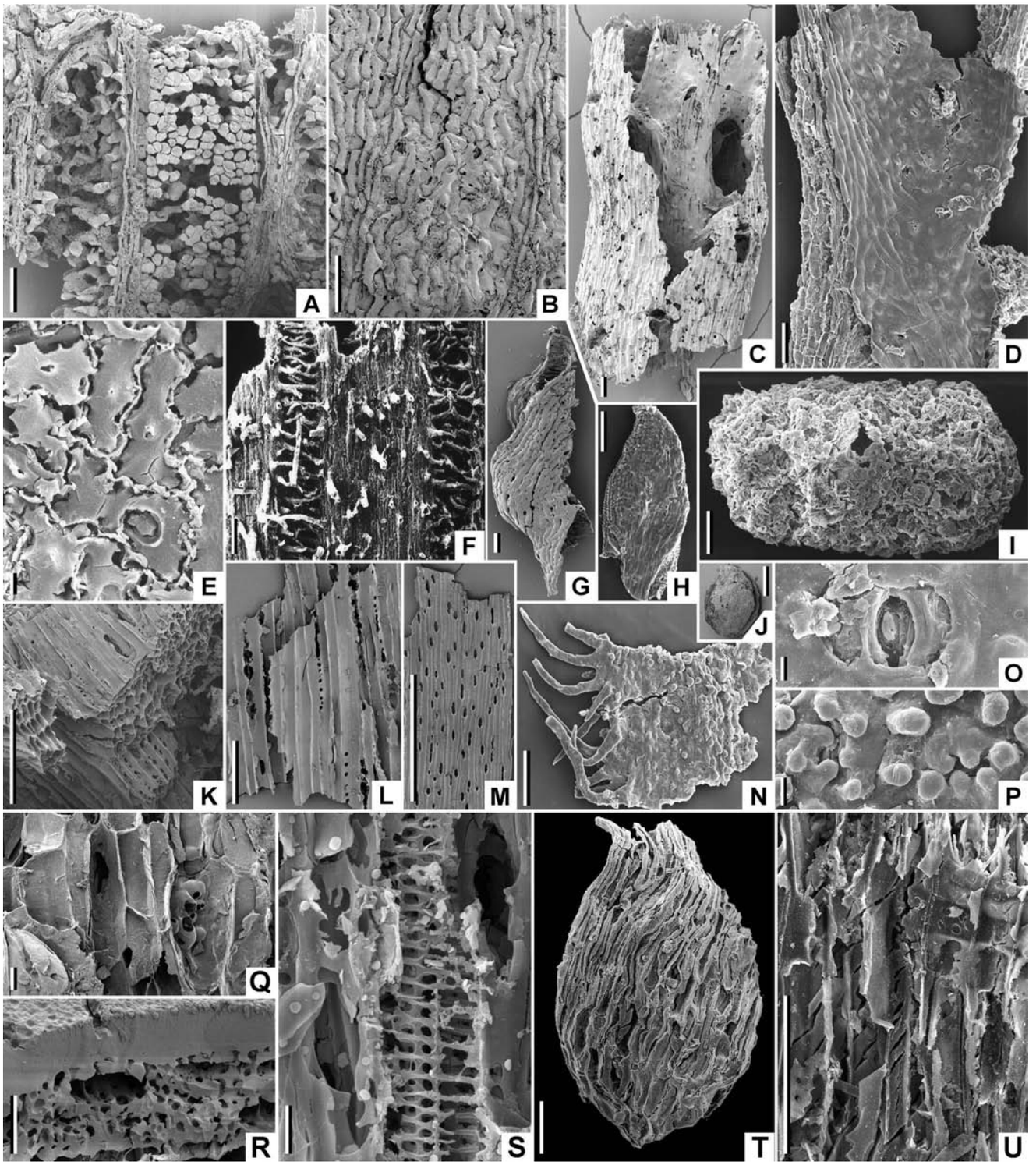

FIG. 8.—SEM images of Permian charcoalified mesofossils from the Amery Group, Radok Lake to Beaver Lake area, Lambert Graben, East Antarctica. **A**) *Glossopteris* leaf fragment with epidermis removed showing veins separating ranks of palisade mesophyll cells (S088062A-15). **B**) Adaxial surface of *Glossopteris* leaf fragment showing slightly sinuous epidermal cells (S087833A-2). **C**) Chambered *Vertebraria* (glossopterid) root (S088043-02). **D**) Exterior of *Glossopteris* leaf fragment showing weakly papillate epidermal cells (S089603-04). **E**) Paradermal section through epidermis of glossopterid leaf showing sinuous-walled cells infilled by homogenous gels (S090230-03). **F**) Abaxial surface of *Noeggerathiopsis* (Cordaitales) leaf fragment showing stomatiferous grooves (NMVP200002A). **G**) Ruptured glossopterid pollen sac (*Arberiella*) with very elongate cells (S087833A-03). **H**) Isolated lycopsid (*Paurodendron stellatum*) microphyll (CPC34970). **I**) Oblong coprolite with pollen and detrital contents (S089603-01). **J**) Isolated seed (S087857-2). **K**) Wood fragment with monoseriate pitting (S088005-2). **L**) Wood fragment in radial longitudinal view with monoseriate

Mesofossil Charcoal in the Bunnerong-1 Well

The measured abundance (percentage) of charcoalified versus non-charcoalified mesofossils per sample and a visual estimate of the relative abundance of charcoal between samples is illustrated graphically (Fig. 11) against a log of the Bunnerong-1 well adapted from Fielding et al. (2019). Although 'organic-rich shale' samples were selected throughout the core, most acid-extracted residues yielded low abundances of mesofossils. Mesofossils are of sparse to moderate abundance in the Changhsingian samples. Mesofossil representation is generally negligible to sparse in the Lower Triassic from the EPE horizon (= base of the *P. crenulata* Palynozone: 805.08 m) to the top of the *P. samoilovichii* Palynozone (413.72 m). Above this level, i.e., within the *A. tenuispinosus* Palynozone, mesofossils are of moderate to high abundance (Fig. 11).

In almost all cases where > 300 organic particles were recovered, charcoal is the dominant mesofossil component. The exceptions are a few samples in the *A. tenuispinosus* Palynozone, in which cuticle fragments and lycopsid megaspores are especially abundant (Fig. 11). Charcoalified plant components throughout the core are represented, in order of decreasing abundance, by wood, megaphyllous leaf fragments, isoetalean microphyll fragments and indeterminate detritus. Sporadic examples of charcoalified unidentifiable seeds, pollen sacs and megaspores are also present. Non-charcoalified mesofossils are represented primarily by leaf cuticle, woody particles, megaspores, and reworked coal fragments. Megaspores increase noticeably in abundance above 587.47 m. Above the base of the *A. tenuispinosus* Palynozone, charcoal levels in these organic-rich samples are commonly only 30–40% compared to > 80% in the pre-EPE Lopingian.

DISCUSSION

Interpreting the Charcoal and Inertinite Records of Eastern Gondwana

As noted by Clark and Patterson (1997), the size profile of charcoal particles in sediments is remarkably consistent, with a ~ 2% decrease in frequency for each 1% increase in grain diameter. Since the three approaches used here to evaluate charcoal representation in Permian–Triassic strata of eastern Australia and East Antarctica employ grains of contrasting size range, they provide notably different results. Point-counting of thin-sections cut through permineralized peat generally yields low values (< 8%) of charcoal as a proportion of peat volume. Counts of inertinite particles in palynological strew slides (with grain sizes of 10–150 μm) predominantly yields values of 10–60% relative abundance for the Lopingian and Lower Triassic. By contrast, charcoal can constitute up to 95% of organic particles in mesofossil residues from the same beds as those sampled for palynology. Nevertheless, each method has its utility.

Permineralized peat or coal ball analysis has the advantage of revealing the proportions of large and minimally transported organic components that contributed to the peat profile and the spatial relationship of plant components within the mire. These studies can also detect discrete fire events and, potentially, their regularity through the interval of peat accumulation. However, permineralized peats are rare and depend on specialized diagenetic conditions for their formation. Palynological analysis has the advantage of surveying a large population of organic particles derived from a broad catchment area, which should provide more robust statistical results of fire frequency in the region. However, because these particles are small and highly fragmented, they are difficult to identify to specific plant groups or organs. Mesofossils are commonly readily identifiable with light microscopy or SEM but acid-extracted residues of this size fraction tend to yield relatively low populations of particles that may not provide statistically robust results. Moreover, depending on the fragility and shape of the organic remains, some particles in this size fraction (both charcoalified and non-charcoalified) may be lost through folding and fragmentation during the sieving process. Our analyses show that all three approaches add value to understanding the frequency of burning and the types of vegetation affected by wildfires through the Permian–Triassic transition. Providing that future studies employ a consistent approach, comparisons of charcoal abundance from other regions and ages with our studied successions should be meaningful.

The Role of Charcoal in Sediments

Charcoal is a relatively inert organic material. It suffers only slow degradation by fungi and bacteria (Saito 1990; Oliver 2011), hence there is probably a taphonomic bias towards its long-term preservation over other plant remains. Long residence times in sediment mean that charcoal probably represents an important carbon sink (Seiler and Crutzen 1980; Bird et al. 2015), although little work has been done to accurately quantify this on a global, long-term basis (Lehmann et al. 2006; Tilston et al. 2016). Various workers have also suggested that charring of peat surfaces or burial of charred particles may be significant in reducing overall methane release from high-latitude wetland and agricultural ecosystems (Dong et al. 2013; Sun et al. 2021). Natural charcoal and modern artificial combustion products (commonly known as biochar) are widely used as additives for remediation of agricultural soils and are said to enhance water retention, raise pH, stimulate microbe activity, improve soil structure and enhance crop yields (Pietikäinen et al. 2000; Jeffery et al. 2011; Tan et al. 2017; Fischer et al. 2018; Palansooriya et al. 2019). However, Brtnicky et al. (2021) noted that the value of such material in some soils is negated by increases in soil salinity, decreased fertility owing to nutrient precipitation in alkaline soils, and changes in the composition of the soil microbiome, among other factors. In the absence of meaningful quantification of charcoal burial through the Permian and Triassic on a global basis, it is difficult to judge the relative role of such material in carbon sequestration in comparison to other processes. Nevertheless, our results suggest that levels of carbon sequestration via burial of charcoal or other terrestrial plant matter were very low in the Early Triassic compared to the Guadalupian–Lopingian in southern Gondwana.

At a much smaller scale, charcoal may have an important role in providing fluid pathways in sedimentary rocks during the early stages of diagenesis. Apart from its relatively inert chemical properties, charcoal is

←

bordered pitting and longitudinal fracturing (S087774-07). **M**) Wood fragment in tangential longitudinal view with rays consisting of a few monoseriate cells (S088062A-02). **N**) Conifer (*Voltziopsis*?) cuticle with prominent trichomes along the margin (S089603-20). **O**) Details of a brachyparacytic stomate on the abaxial surface of a possible Umkomasiaceae leaf fragment (S089574-06). **P**) Heavily papillate epidermal cells and stomata on abaxial surface of a possible peltasperm leaf fragment (S089719). **Q**) Pith cells of a gymnosperm with one blistered cell lining (S088043-2). **R**) Transverse fracture of seed coat showing homogenized cell walls (S087838-02). **S**) Fern or lycopsid tracheids with scalariform pitting and homogenized cell walls (S088072-19). **T**) Pollen sac wall showing contractional separation of cell walls along middle lamellae (S090233-10). **U**) Wood with remnants of cross-field pitting and *en echelon* contractional fracturing of tracheids (S089891-02). Note: A–C, E–G, J–M uppermost bed of the Toploje Member, at sites PCM92/1 (E, J, U), PCM92/2 (B, C, G, Q, R), PCM92/3 (F, K), PCM92/8 (A, M), PCM 92/9 (L), PCM 92/15 (S), see Fig. 4; D, N from top of Glossopteris Gully Member (level PCM95/26A), H from upper McKinnon Member (level 95/12), O from middle Grainger Member (level PCM95/20), P from uppermost McKinnon Member (level 95/4), and T from McKelvey Member (level PCM95/88): sampling levels are those of McLoughlin and Drinnan (1997a; 1997b) and Lindström and McLoughlin (2007). Scale bars = 1 mm for M; 500 μm for J; 100 μm for A–D, F–I, K, L, N, T, U; 10 μm for E, O, P–S.

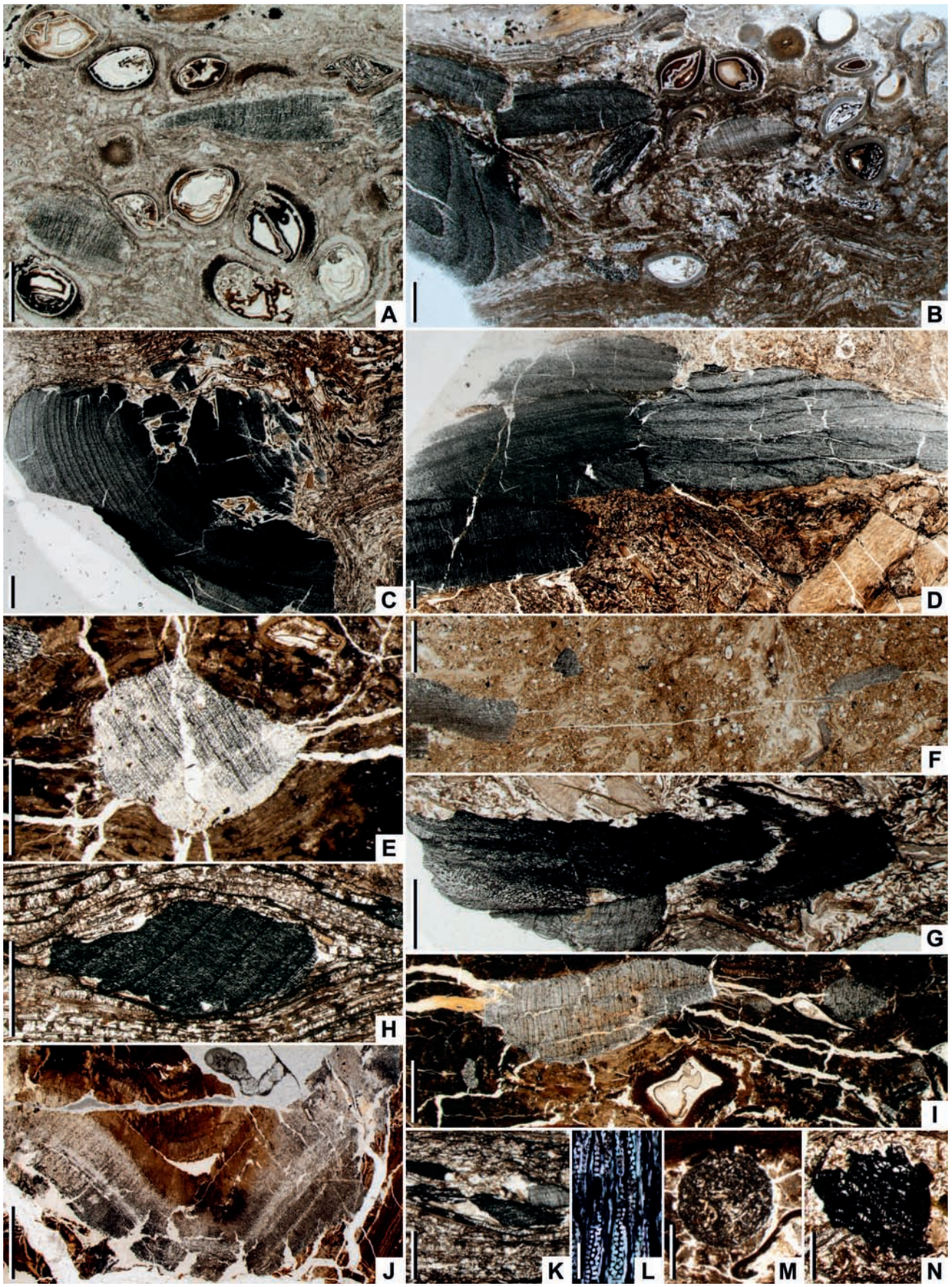

FIG. 9.—Charcoal in thin-sections of Permian permineralized peat from eastern Gondwana. **A**) Subrounded charcoal fragments in seed-rich microfacies (AMF12048g-2). **B**) Subangular charcoal fragments in seed-rich microfacies bracketed by leaf-rich microfacies (AMF92048k-2). **C**) Large charcoalified wood fragment retaining growth rings

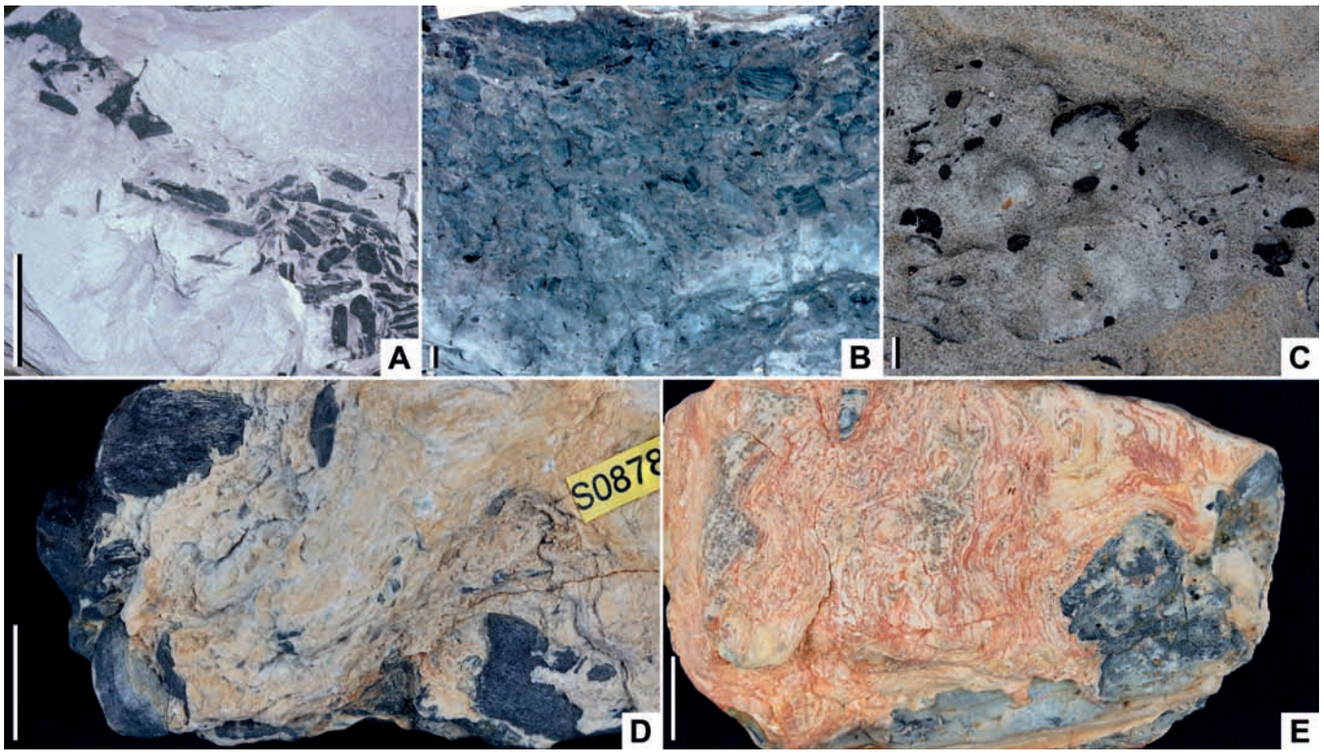

FIG. 10.—Examples of macroscopic charcoal occurrences in Guadalupian–Lopingian continental strata of eastern Gondwana. **A**) Poorly sorted band of large, mostly angular, charcoalified wood fragments within a channel sandstone above the Pollux coal seam, Rangal Coal Measures, South Blackwater Mine, central Bowen Basin, Australia. **B**) Thick accumulation of subrounded charcoal fragments in a splay deposit above the Wallarah coal seam, Moon Island Beach Formation, at Ghosties Beach, northern Sydney Basin, Australia. **C**) Mostly rounded and isolated charcoal clasts within volcanigenic channel sandstones between the lower and upper Pilot coal seams, Boolaroo Subgroup, Newcastle Coal Measures, at Swansea Heads, northern Sydney Basin, Australia. **D**, **E**) Large charcoalified wood fragments within leaf-rich and laminated detrital permineralized peat blocks from the top of the Toploje Member, Bainmedart Coal Measures, Radok Lake area, East Antarctica (S087819 and S087817, respectively; site PCM92/9, see Fig. 4). Scale bars = 30 cm for A, 10 mm for B–E.

physically robust and resists compaction to a much greater degree than other buried plant matter (Fig. 9C, 9H). Charcoal (or fusinite) particles retain an open cellular structure even up to the higher grades of bituminous coalification (Stach 1982), which, depending on the geothermal gradient, generally requires burial to depths of $>$ 1500 m (Teichmüller and Teichmüller 1982). Thus, charcoal provides porosity, pathways for fluid migration, and sites for deposition of authigenic minerals, such as pyrite and kaolinite, within much of the shallow sedimentary column. Moreover, in the Permian permineralized peats of Antarctica and eastern Australia, the differential compaction around charcoal particles in tandem with their retention of high porosity has led to the focusing of fractures around such grains that act as pathways for the movement of subsequent silica-rich fluids and sites for chalcedony precipitation (Fig. 9E, 9I).

The Role of Fire in Late Permian Glossopterid-Dominated Ecosystems

Fire was clearly common in Gondwanan forest ecosystems throughout the Permian Period, based on the distribution of dispersed charcoal in continental siliciclastic strata (Jasper et al. 2013, 2017; Degani-Schmidt et al. 2015). Macro-charcoal, either as isolated clasts or thick bands, is common in a range of continental sedimentary facies in eastern Gondwana. Macro-charcoal accumulations are particularly abundant in some fluvial channel and splay sandstones (Fig. 10A, 10B), and in beds bracketed by tuffaceous deposits (Fig. 10C). The numerous bands of charcoal identified in permineralized peats of Gondwana (Holdgate et al. 2005; Slater et al. 2015; McLoughlin et al. 2019; Figs. 9A–9G, 9I, 10D, 10E) and inertinite particles in bituminous coal (Glasspool 2000; Ayaz et al. 2016b; Jasper et al. 2017; Benicio et al. 2019) suggest that wildfires were regular events

←
in leaf-rich microfacies (S089948-01). **D**) Large fractured charcoalified wood fragment in microfacies dominated by coarse organic detritus (S090232-01). **E**) Large porous charcoalified wood fragment forming the focus of radial chalcedony-filled fractures (S124952-02). **F**) Small angular charcoalified wood fragments embedded in finely macerated organic debris (S090231-08). **G**) Large charcoalified wood fragment embedded in matrix dominated by roots and coarse organic debris (S089945-01). **H**) Subrounded charcoalified wood fragment draped by strongly compacted leaf mats (S089950-03). **I**) Band of woody charcoal forming the focus of extensive chalcedony-filled fracturing (S089828-04). **J**) Transverse section of permineralized wood with charcoalified and fractured outermost layers (lower) grading into non-charcoalified xylem tissue (upper) (S124927-05). **K**) Angular charcoalified leaf and wood fragments (S089959-02). **L**) Charcoalified *Agathoxylon* or *Australoxylon* (glossopterid) wood in radial longitudinal section showing multiseriate bordered pitting (AMF92048k-1). **M**) Charcoalified invertebrate coprolite (S089862-03). **N**) Oblique section through a charcoalified lycopsid (*Paurodendron stellatum*) axis (S089946-01). Notes: A, B, L from lower Wilton Formation (Wuchiapingian), Thirroul Beach, southern Sydney Basin, eastern Australia. C, D, F–H, K, N from uppermost Toploje Member, Bainmedart Coal Measures (Guadalupian), Radok Lake area, Lambert Graben, East Antarctica (C, D, G, H, K, N from site PCM92/9; F from site PCM92/3, see Fig. 4). E, I, J, M from Fort Cooper Coal Measures (lower Changhsingian), Homevale, northern Basin, eastern Australia. Scale bars = 2 mm for A–D, F–I; 1 mm for E, K, M, N; 50 μm for L.

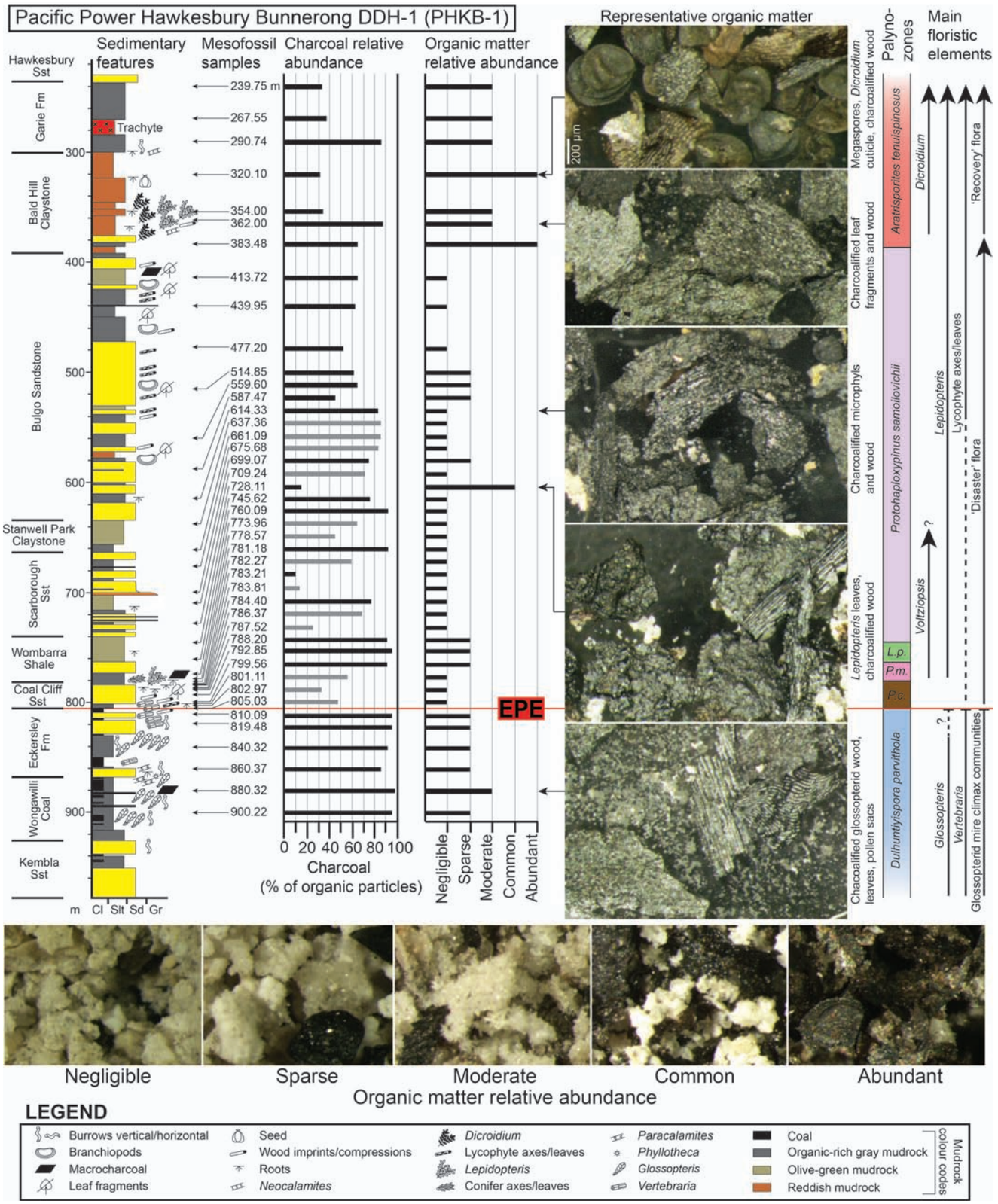

FIG. 11.—Graphic log of Pacific Power Hawkesbury Bunnerong DDH-1 (Bunnerong-1) bore core (after Fielding et al. 2019) indicating the stratigraphic positions of mesofossil samples, and showing (in columns progressively to the right): the relative abundance of charcoal as a percentage of organic particles; the relative abundance of organic particles (based on qualitative visual estimates according to the images at the base of the diagram); images of representative suites of organic particles; the palynostratigraphic zones of the core; and the ranges of key plant macrofossil taxa and floristic stages. Abbreviations: *P.c.* = *Playfordiaspora crenulata*; *P.m.* = *Protohaploxypinus microcorpus*; *L.p.* = *Lunatisporites pellucidus*.

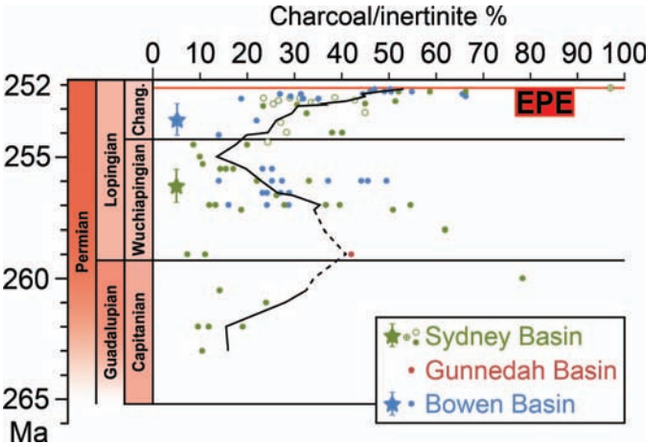

FIG. 12.—Mid- to late Permian charcoal/inertinite abundances of eastern Australia (relative to total organic content). Line indicates coal inertinite 5-point running mean of 100k year time bins. Abbreviations and symbols: Chang. = Changhsingian Stage; EPE = terrestrial end-Permian extinction event; crossed circle = micro-charcoal peak from the northern Sydney Basin (Vajda et al. 2020); empty circles = inertinite from siliciclastic samples (Bunnerong-1, this study); stars = charcoal from permineralized peats (this study, error ranges reflect the uncertain stratigraphic placement of these assemblages); dashed line indicates an interval of sparse data coverage. Data compiled by Diessel (2010), Glasspool and Scott (2010), Glasspool et al. (2015) and this study (see Online Supplemental File Table S2).

even in high-latitude glossopterid-dominated Permian mire systems of consistently humid environments. The subrounded to angular nature of much of the charcoal within the permineralized peats of this study suggest only a modest degree of transport before incorporation in the peat profile. These grains may have been winnowed, abraded, and transported by water to form local accumulations on the peat surface. We did not find any cases of gradational charring of the peat laminae or sharply incised charred surfaces of the peat matrix that would indicate burning of the local peat profile *in situ*. Most of the charcoalified remains appear to represent either charred subaerial plant components of, e.g., canopy fires, or material rafted into the peatland setting from adjacent areas.

Although we cannot exclude widespread burning of the *in situ* peat surface as an ecological process in Gondwanan mires, there seems to be little evidence for this in the three permineralized deposits studied here. One example of a charcoalified glossopterid root (Fig. 8C) indicates at least some burning of subterranean plant components. Given that glossopterids were specifically adapted to growth in consistently waterlogged substrates via the possession of aeration systems in their chambered roots (Neish et al. 1993), mires were probably less subject to fires than vegetation growing on better-drained mineral soils adjacent to the peatland. Nevertheless, the generally consistent representation of charcoal among the three peat profiles suggests that fire was a regular factor within or adjacent to mires that developed in the Permian cool, humid, high-latitude settings of southern Gondwana. Middle to upper Permian bituminous coals of eastern Australia and Antarctica generally have high representations of inertinite macerals compared to Paleozoic coals of the Northern Hemisphere (Hunt 1982, 1989). As in the permineralized peat samples studied here, fusinite and semifusinite particles commonly occur in bands of discrete particles within these coals (Diessel and Smyth 1995), indicating an origin as transported charcoal rather than representing charred peat surfaces.

Coal deposits show a distinct global increase in inertinite from the middle to late Permian (Diessel 2010; Glasspool and Scott 2010; Glasspool et al. 2015) indicating increasing wildfire prevalence in or around the peat-forming wetlands. The eastern Australia compilation of coal-derived inertinite (Fig. 12; Online Supplemental File Table S2) reflects the general increase from the Capitanian (mean = 23.7%) through the Wuchiapingian (28.9%) and into the Changhsingian Stage (37.7%). At present, there are insufficient data to confidently infer the inertinite trends prior to the mid-Wuchiapingian; after this interval, however, rather than a monotonic increase, there is a distinct inertinite dip during the late Wuchiapingian–early Changhsingian (Fig. 12). This dip may be supported by the low abundance of charcoal (5%) from the early Changhsingian Homevale permineralized peat, but we caution that the measured proportions of charcoal are generally lower in permineralized peats than in mesofossil or palynofloral assemblages macerated from mudrocks. For example, although macro-charcoal fragments are obvious in the Wuchiapingian Thirroul Beach permineralized peat, the measured relative abundance is low (4.5%) for this interval based on other sampling methods. A fire-prone Changhsingian interval is supported here by high inertinite relative abundances (34–49%) from the shale assemblages (pre-EPE Changhsingian means, range of all successions), with a general increase throughout the stage. This rising inertinite trend is reflected by the coal-derived compilation of eastern Australia, suggesting that shale/siltstone- and coal-derived assemblages provide consistent and complementary records of wildfire activity. The very high inertinite abundances (63–64.5%) from the uppermost Permian coal (Bulli Coal) indicate regular wildfires in the humid lowlands (Fielding et al. 2021) immediately prior to the EPE.

The regional increase in wildfire prevalence throughout the late Permian was likely due to significant changes in climate but catalyzed by intermittent local ignition sources. The Permian volcanic arc along the continent's eastern margin, the New England Orogen (Jones et al. 1987; Jessop et al., 2019), would likely have played a role in initiating late Permian wildfires in the region. This has been suggested as an ignition source for a major wetland wildfire event recorded from Wuchiapingian coal measures of the Sydney Basin (Glasspool 2000). Permian volcanism in this region peaked slightly before the end of the period (Jones et al. 1984; Veevers et al. 1994; Jessop et al. 2019), as evident by the numerous and voluminous volcaniclastic deposits (Fig. 3). These would have provided ample opportunities for initiating wildfires in the region, above the background occurrence of lightning strikes, which have likely served as perennial wildfire triggers since the evolution of the first land plants (Cope and Chaloner 1985; Scott and Jones 1994).

The climate has a decisive role in both the flammability of the vegetation and, once ignited, determining the spread and duration of wildfires (Jolly et al. 2015). At sufficiently high atmospheric oxygen concentrations (pO_2), even vegetation with high-moisture content is susceptible to burning (Watson et al. 1978; Wildman et al. 2004; Belcher et al. 2010; Watson and Lovelock 2013); hence, elevated pO_2 has been proposed as a leading cause for high wildfire prevalence in the coal-forming wetlands of the late Permian (Glasspool et al. 2015). Most model- and proxy-based estimates of late Permian pO_2 infer levels above the modern value of 21% (Krause et al. 2018; Brand et al. 2021, and references therein). Taking the inertinite record as a proxy for pO_2 (Glasspool and Scott 2010; Glasspool et al. 2015), the age-calibrated records of eastern Australia (Fig. 4) would indicate increasing levels of atmospheric oxygen throughout the Changhsingian. However, there may have been regional climatic (e.g., seasonal drought) or volcanic influences that affected this inertinite trend.

There is no irrefutable evidence that glossopterid gymnosperms, the dominant plants of eastern Gondwana during the late Permian, had reproductive strategies specifically tied to fire events, such as is the case for various modern plant taxa and vegetation types (Kruger 1983; Williams 2000; Marod et al. 2002; Rowe et al. 2017). Although some gymnosperm groups may have had traits for fire-triggered seed dispersal since the Carboniferous (He et al. 2016), the oldest direct fossil evidence of this fire-adaptive strategy is from the mid-Cretaceous (Mays et al. 2017). Nevertheless, the production of large numbers of small seeds by many glossopterid taxa, and vegetative regeneration from epicormic buds and

possibly lignotubers (Decombeix et al. 2010; McLoughlin and Prevec 2021) were strategies that may have aided rapid recovery after fires and led to the growth of uniform-age cohorts of trees in the vegetation, as is the case for various modern tree taxa adapted to regular fire cycles (Gill 1981; Pausas et al. 2004). Similarly, the thick layer of insulating bark found on some Antarctic glossopterids has been postulated as an adaptation to abiotic environmental factors, including fire (Decombeix et al. 2016). Almost all glossopterids were deciduous (McLoughlin 2011, 2021; Gulbranson et al. 2014), and this regular foliar shedding resulted in seasonal leaf litter build-up, reflected by near-monospecific leaf-mats (Gould and Delevoryas 1977; Retallack 1980; McLoughlin 2011). This would likely "have promoted regular surface fires but without resulting in tree mortality" (Glasspool et al. 2015, p. 8). The occurrence of low-intensity fires is supported by the presence of at least one small axis preserved in the Homevale permineralized peat having an outer rim of charcoalified tissues enveloping non-charred interior wood (Fig. 9J). The above combination of characteristics likely provided selective advantages to glossopterids during the regular fire events of the late Permian and may in part explain the longevity of the *Glossopteris* biome within the humid but fire-prone high southern latitudes. However, studies of modern vegetation show that an increase in fire frequency can severely deplete seed set and seedling recruitment, ultimately leading to marked changes in vegetation structure (Cury et al. 2020).

Wildfires of the End-Permian Ecosystem Collapse: A Cause, a Consequence, or a Combination?

The Siberian Traps Large Igneous Province is consistently implicated as the ultimate cause of continental biodiversity loss during the end-Permian extinction event (Wignall 2001; Bond and Grasby 2017). A cornerstone of this consensus is that changing climate (*sensu lato*, including atmospheric composition), as a result of igneous activity, served as the intermediate cause of the global extinctions. Acid rain, driven by voluminous magma-derived emissions of sulphur dioxide (SO_2) and carbon dioxide (CO_2; Black et al. 2018), has been proposed as a cause of additional stress on late Permian continental biotas (Sephton et al. 2015). However, this may not have played a large role in Gondwana since the distribution of acid rain was likely restricted to the Northern Hemisphere (Black et al. 2014). The copious release of halocarbons (e.g., chloromethane, CH_3Cl) from Siberian Traps contact metamorphism (Svensen et al. 2009, 2018) may have weakened the ozone layer, leading to dangerous levels of radiative stress from UV-B (280 to 315 nm) for organisms on the Earth's surface (Beerling et al. 2007). UV-B experiments on plant reproductive organs have demonstrated reduced fertility in gymnosperms (Benca et al. 2018), and relatively high proportions (above background levels of about 3%: Lindström et al. 1997) of deformed pollen or plant spores from the end-Permian extinction interval have been interpreted as the teratological effects of elevated UV-B on land plants (Visscher et al. 2004; Foster and Afonin 2005). However, while the degree of ozone depletion was likely highest at polar latitudes (Black et al. 2014), it is not clear whether the increased radiative stress was sufficient to biologically impact the *Glossopteris* biome, as these regions also receive the lowest doses of incident UV-B, particularly at low altitudes (Beckmann et al. 2014), such as those of the late Permian coastal wetlands of eastern Australia. Toxicity by metals has been proposed as another stressor on EPE terrestrial ecosystems (Grasby et al. 2020; Chu et al. 2021). Anomalously high concentrations of mercury (Hg) and other potential metal toxins have been reported from continental sections encompassing the EPE (Shen et al. 2019; Chu et al. 2020), the sources of which were likely Siberian Traps volcanic emissions (Sanei et al. 2012), destabilization of soils (Grasby et al. 2020), and/or oxidation of terrestrial biomass (Dal Corso et al. 2020). Such toxicity has been indicated as another potential source of the increase in deformed spores/pollen from various EPE successions (Chu et al. 2021).

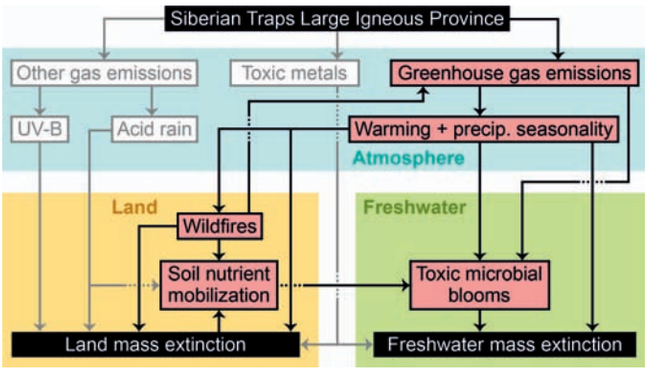

FIG. 13.—Proposed conceptual model of continental biodiversity loss during the end-Permian extinction event. Widespread wildfires and deforestation serve as the catalysts for a series of deleterious events, including soil nutrient loss and harmful freshwater microbial blooms. Red boxes and black arrows indicate drivers and causal pathways that have been identified from the basins of eastern Australia. Arrow from 'land mass extinction' to 'soil nutrient mobilization' represents the impacts of deforestation. Adapted from Wignall (2001) and Bond and Grasby (2017).

Regardless of the cause(s), deformed spores/pollen are rare in the Southern Hemisphere (Visscher et al. 2004) and no anomalous abundances of these have yet been reported from Australia, although not for lack of searching. This suggests that UV-B- or toxin-induced stress in late Permian plants was not: (1) universally expressed as pollen or spore teratogenesis and/or (2) a global phenomenon.

Greenhouse gases are another class of climatic stressors derived from the Siberian Traps that likely contributed to the collapse of late Permian Gondwanan ecosystems (Fig. 13). Their global distribution and effects on other climate variables (e.g., temperature, precipitation) have been long-established (e.g., Arrhenius 1896; see Fleming 1998). Climate reconstructions of the EPE consistently indicate enormous emissions of greenhouse gases from the Siberian Traps via both contact metamorphism with hydrocarbon-rich sedimentary strata (Black et al. 2018) and direct volcanic outgassing (Svensen et al. 2018). Recent estimates of atmospheric CO_2 concentrations revealed an increase in the earliest Triassic by a factor of six from pre-EPE levels (Wu et al. 2021). This increase in CO_2 is estimated to have occurred within tens of millennia (Burgess et al. 2014; Wu et al. 2021), and would have been the primary force behind the inferred rise in temperature of 6–12°C in the tropics (Sun et al. 2012; Chen et al. 2020) and 10–14°C in the high-latitude basins of eastern Australia (Frank et al. 2021). The EPE temperature increase has been linked to enhanced seasonality in precipitation across eastern Gondwana (Fielding et al. 2019; Frank et al. 2021). Elsewhere in Gondwana, EPE precipitation regime changes have been inferred from the occurrence of continental Fe-rich mudrock ('red-bed') deposits in India (Dutta 2002; Shah 2021) and southern Africa (Smith and Botha-Brink 2014; Gastaldo et al. 2015). The rapid onset of seasonally dry conditions, combined with elevated temperatures and high late Permian oxygen levels, would have greatly enhanced the potential flammability of the peat-forming wetland vegetation of Gondwana.

The near-synchronous peaks in inertinite abundances across the Sydney Basin immediately following the extirpation of peat-forming vegetation (62–65%) support an increase in wildfire activity in eastern Gondwana during or immediately after the EPE (Vajda et al. 2020). Elevated occurrences of wildfire concurrent with, or soon after, the EPE have also been inferred from the low-latitude peat-forming alluvial plains of China (Shen et al. 2011b; Zhang et al. 2016; Chu et al. 2020; Cai et al. 2021b), suggesting that, given the regional differences in climates and biotas, this fire-prone interval was caused by a global shift in climate (e.g., greenhouse gas-driven warming). However, the fossil records of Australia (this study)

and China (Chu et al. 2020; Cai et al. 2021a) both reveal high inertinite/charcoal abundances up to several meters above the uppermost Permian coals, representing a substantial duration after the primary phase of ecosystem collapse. Rather than indicating a direct cause of extinctions, high abundances of charcoal in the aftermath of the EPE may partly derive from the combustion of peat biomass that had died from other causes. The burn probability of this biomass would have been enhanced owing to the high pO_2 of the late Permian (Yan et al. 2019), and increased temperature and seasonally dry conditions. Furthermore, the inert nature of charcoal (Jones and Chaloner 1991) makes it resistant to chemical breakdown, enhancing its longevity in the sedimentary cycle. The detection of reworked micro-charcoal is confounded by its tendency to splinter into lath-shaped fragments (Scott 2010) rather than become rounded like many other common sedimentary particles. The sparse vegetation in the immediate aftermath of the EPE (Mays et al. 2020) led to a paucity of autochthonous plant remains (McLoughlin et al. 2021); hence, reworked pre-EPE charcoal could be over-represented in this interval. More highly resolved age controls on strata around the EPE horizon would build a much stronger case for the causal relationship and timing between wildfire activity and continental ecosystem collapse.

Today, changes in fire regimes, expressed by an increase in fire frequency or intensity, threaten thousands of plant and animal species with extinction (Kelly et al. 2020). In regions of high rainfall, a reduction in seasonal precipitation has led to a synergistic increase in direct tree mortality and fire frequency (Brando et al. 2014, 2019). A recent rise in fire activity in the Brazilian Pantanal region, South America, demonstrates that anomalous warming and short-term reduction in precipitation is sufficient to significantly promote and sustain wetland wildfires (Marengo et al. 2021). Moreover, fires in modern peat-forming swamps have resulted in total tree cover loss (Goldammer and Seibert 1990) and mortality rates of $\geq$ 98% (Johnson 1984). Increased fire frequency has also provided intolerable stress on the reproductive cycles of trees with fire-adaptive traits (*sensu* Keeley et al. 2011) leading to forest structure changes in Australia (Fairman et al. 2016), Canada (Whitman et al. 2019), Russia (Barrett et al. 2020) and the USA (Turner et al. 2019). These recent examples demonstrate that changes in wildfire regime can act as a threat to wetland vegetation and can directly impose rapid ecosystem changes during warming intervals. Furthermore, modern climate-related fire regime changes are occurring across disparate localities (Kelly et al. 2020), indicating an apparent global distribution of this biodiversity stressor, and mirroring the enhanced wildfire prevalence in both the low- and high-latitude wetland basins of the late Permian.

Enhanced fire activity and the occurrence of sporadic megafire events also impact the structure of animal communities. Recent megafires have witnessed catastrophic animal losses in Australia (Lewis 2020) and central South America (Tomas et al. 2021). In these communities, survival is favored for animals with a fossorial lifestyle, since temperature changes are negligible in burrows that extend more than 5 cm below the soil surface (Recher et al. 2009; Costa et al. 2013). In addition, modern observational studies of echidnas (Tachyglossidae), semi-fossorial monotremes, have revealed high wildfire survival rates, owing largely to their heterothermy, whereby they undergo an interval of energy-conserving torpor following a fire (Nowack et al. 2016). By inference, abruptly enhanced land surface temperatures, sharp changes in moisture levels and elevated fire occurrences around the EPE may have collectively favored the survival of (semi-)fossorial and heterothermic vertebrates through this biotic crisis. In support of this hypothesis, it is noteworthy that many (and perhaps a majority) of taxa in the rich vertebrate faunas of the Permian–Triassic transition in the Karoo Basin (South Africa) and in surrounding regions of Gondwana adopted a fossorial habit (Groenewald et al. 2001; Smith and Botha 2005; Gastaldo and Rolerson 2008; Sidor et al. 2008; Bordy et al. 2011; Bordy and Krummeck 2016; Botha-Brink 2017; Botha et al. 2020). Such behaviors may have provided access to more stable micro-environments and reduced rates of juvenile mortality in brood chambers (McLoughlin et al. 2020; Smith et al. 2021).

In addition to direct ecological stress to life on land during the end-Permian event, enhanced wildfire would have influenced the atmosphere and hydrosphere. Wildfires contribute the equivalent of 22% of modern CO_2 emissions from burning fossil fuels (van der Werf et al. 2017) and CO_2 emissions from one recent extreme fire event were more than double the predicted estimate (van der Velde et al. 2021). Peat burning has been suggested as a significant contributor to CO_2 release during the EPE (Glasspool et al. 2015) and other hyperthermal events (e.g., Paleocene–Eocene thermal maximum, Kurtz et al. 2003; Toarcian oceanic anoxic event, Finkelstein et al. 2006). These fire-driven greenhouse gas emissions would be an important climatic feedback element during hyperthermal events, such as the EPE (Fig. 13). Fires also greatly enhance nutrient influx into regional freshwater or marine environments via soil runoff and dispersal of suspended ash (Smith et al. 2011). Based on studies of recent marine and riverine/lacustrine algal blooms in the wake of major modern wildfire events (Ranalli 2004; Tang et al. 2021), we hypothesize that the elevated fire regime at the close of the Permian and subsequent nutrient influx may have contributed to eutrophication and the proliferation of micro-organisms (e.g., bacteria and algae) in aquatic ecosystems (Fig. 13). In turn, these microbial 'blooms' may have suppressed the recovery of freshwater ecosystems from the end-Permian extinction event until well into the Early Triassic (Mays et al. 2021a).

The impact of enhanced wildfire on the broader end-Permian landscape and sedimentation processes can only be inferred in broad terms. Muir et al. (2015) noted that there is generally a poor understanding of how fires have affected the geological record over long timescales. At short timescales, however, inferences can be drawn from studies of modern settings. The impacts of fires on modern landscape and sedimentation processes depend strongly on the local geomorphology and the magnitude of, and interval between, the wildfire and subsequent precipitation events (Vieira et al. 2015; Wu et al. 2020). Vegetation loss by fires in modern continental settings, generally leads to altered moisture infiltration regimes (Wieting et al. 2017), increased runoff (De Bano 2000), destabilization and erosion of soils (Meyer et al. 2001; Shakesby and Doerr 2006; Vieira et al. 2015), and changes in sedimentation dynamics, such as alluvial fan accretion, channel bar aggradation, and activation of debris flows (Florsheim et al. 1991; Benda et al. 2003; Ryan et al. 2011; Rengers et al. 2017). The notable concentrations of charcoal in many sandy to gravelly channel and crevasse splay deposits throughout the Lopingian alluvial systems of eastern Australia (Fig. 10A–10C; Vajda et al. 2020; Fielding et al. 2021) probably reflect locally enhanced soil erosion and charred litter transport after episodic fire events.

A Depressed Early Triassic Fire Regime

Owing to its anomalously low charcoal and inertinite abundances, Lower Triassic sedimentary records have been described as exhibiting a 'charcoal gap' (Uhl et al. 2010). Reports of charcoal are exceptionally rare (Uhl et al. 2008), and when found, tend to be restricted to single stratigraphic horizons (Wan et al. 2021). Historically, a contributor to this gap was an absence of data. Since inertinite abundances are primarily derived from coal measures (e.g., Diessel 2010; Glasspool and Scott 2010; Online Supplemental File Table S2), these data have been extremely scarce from Lower Triassic deposits, caused by a near-total absence of coal in the global stratigraphic record for several million years following the EPE (the 'coal gap'; Veevers et al. 1994; Retallack et al. 1996). Similarly, no permineralized peats are available from the studied basins to assess *in situ* charcoal content of wetland settings, owing to the dearth of Early Triassic peat-forming ecosystems. However, the concordant pre-EPE Lopingian coal and shale inertinite records from the Sydney Basin indicate that shale-derived inertinite abundances suffice in the absence of coal. As such, the

present study helps to fill the gap in our knowledge of Early Triassic wildfire activity.

Despite the apparently warm and seasonally dry conditions affecting both East Antarctica and eastern Australia during the Early Triassic (McLoughlin and Drinnan 1997b; McLoughlin et al. 1997; Cantrill and Webb 1998; Retallack et al. 2011), the relatively low Lower Triassic mesocharcoal and inertinite abundances suggest that the fire regime was suppressed relative to that of the Lopingian. Although the mesofossil record from the Bunnerong-1 core reveals generally low abundances of organic matter in strata from the EPE horizon to near the Smithian–Spathian boundary (~ base of the Bald Hill Claystone; ~ base of the *Aratrisporites tenuispinosus* Palynozone), charcoal was recovered from every sample. Although the relative proportion of charcoal in this interval remains high, the small number of organic particles in general (< 300 in many samples) means that absolute charcoal concentrations are low for this interval. Similarly, the low post-EPE inertinite abundances (pre-EPE mean = 34–49%; post-*P. crenulata* Zone mean = 18.6–31%; Fig. 5) indicate a reduction in wildfire activity for at least three million years (until the Spathian substage) following the collapse of continental ecosystems. Collectively, these data support an Early Triassic 'charcoal depression'.

In addition to the historic lack of attention, three additional reasons have been advanced for the paucity of Early Triassic charcoal (Uhl et al. 2010; Abu Hamad et al. 2012): (1) preservation biases; (2) low atmospheric oxygen concentrations; and (3) a scarcity of biomass to act as fuel. The earliest Triassic climatic conditions may have led to continental environments with low potential for the preservation of charcoal. The post-EPE formation of 'red-beds' in some regions may have decreased the preservational potential of charcoal (Belcher and McElwain 2008). Although eastern Australia underwent a change in precipitation regime, it was spared the intensity of drought conditions that have been inferred for some regions (e.g., Smith and Botha-Brink 2014; but also see Gastaldo et al. 2020). Instead, organic (micro)fossils, including inertinite and mesocharcoal, are well-preserved in the dark, carbonaceous shales of eastern Australia, and red-bed deposits are absent until the mid-Olenekian (c. 250–249 Ma; Fig. 3).

Low atmospheric oxygen concentration (pO_2) has been proposed as a contributor to the apparent reduction in wildfire activity during the Early Triassic. Early climate models estimated Early Triassic pO_2 levels similar to (Bergman et al. 2004) or lower (Berner 2005, 2006, 2009) than today. A consequence of reduced pO_2 for the Early Triassic would be lower wildfire activity (Glasspool and Scott 2010; Glasspool et al. 2015) as this would reduce the probability of ignition and propagation (Belcher et al. 2010). Proxy-based approaches have generally noted the sparse records for this interval (e.g., Glasspool and Scott 2010) that, nevertheless, generally indicate low Early Triassic charcoal abundances, which have been inferred to imply a reduction in pO_2. More recent climate models, however, generally estimate only a modest reduction in pO_2 from pre-EPE levels, and retention at consistently higher values than modern pO_2 for the Early Triassic (Krause et al. 2018; Lenton et al. 2018; Mills et al. 2021), suggesting that oxygen was not the primary limiting factor to fire ignition and spread.

We propose that a scarcity of flammable biomass, as a function of the vegetation type, likely played a pivotal role in the low charcoal/inertinite abundances for the Early Triassic. In contrast to the dense, deciduous, broad-leafed, peat-forming mire vegetation of the Lopingian, eastern Gondwana was characterized by sparse, open woodlands for millions of years following the EPE (Mays et al. 2020; McLoughlin et al. 2021). This is supported by the significant drop in plant spore-pollen concentrations (Fig. 5) and weakly developed root systems in paleosols of the Sydney Basin (Retallack 1999). Early Triassic floras of both studied regions were initially dominated by *Lepidopteris* (Peltaspermales) and *Voltziopteris* (Voltziales) gymnosperms (Retallack 1980, 2002; McLoughlin et al. 1997), which likely formed a low woody sclerophyllous vegetation of open character (Retallack 2018). With few intervening ground-stratum plants, and low total biomass, the earliest Triassic vegetation may have endured lower frequencies of wildfires compared with the high-biomass Permian forests, albeit that the glossopterid communities grew under cooler and more consistently humid conditions. Once ignited, the sparseness of the vegetation would have severely limited the spread of these fires (Alexandridis et al. 2008). Later in the Early Triassic, the low herbaceous to shrubby vegetation dominated by opportunistic cormose pleuromeian lycopsids that occupied seasonal wetlands may, similarly, have been affected by only intermittent fire events. It is likely that fire only regained prominence in the landscape as denser complex multi-tiered vegetation dominated by woody umkomasialean gymnosperms (e.g., *Dicroidium*) developed near the end of the Early Triassic and diversified through the remainder of that period. Indeed, possible fire scars (and cambial recovery) have been reported on gymnosperm woods from the Fremouw Formation of the Transantarctic Mountains (Jefferson and Taylor 1983; Putz and Taylor 1996), and macro-charcoal bands become obvious in sandstone bodies of eastern Australia in the Nymboida Coal Measures (Holmes and Anderson 2013) indicating a return to more fire-prone vegetation in the region by the Middle Triassic.

CONCLUSIONS

Long-term wildfire trends of the late Permian (Lopingian) to Early Triassic were compiled for the high southern latitudes of eastern Gondwana (Antarctica and eastern Australia) based on charcoal and inertinite occurrences in palynological, mesofossil, and macrofossil assemblages. Each data set yielded different quantitative results but provided complementary information on the distributions and botanical origins of macro- and micro-charcoalified fossil remains.

Late Permian assemblages consistently indicated fire-prone conditions in the peat-forming mire ecosystems, fueled by dense biomass and promoted by high atmospheric oxygen. The primary wetland plants of the region, the glossopterids, apparently had fire-adaptive traits that may have served to sustain their dominance in the Permian high southern latitudes throughout the interval. A compilation of age-calibrated inertinite records from across eastern Australia shows a distinctive increase during the final stage of the Paleozoic (Changhsingian) until the end-Permian extinction event (EPE).

A peak in charcoal and inertinite abundances supports increased wildfire activity concurrent with, or soon after, the continental EPE (c. 252.2 Ma). Evidence for enhanced wildfires in both high- and low-latitude regions (Australia and China, respectively) suggests that it was caused by a shift in global climate, ultimately driven by the Siberian Traps Large Igneous Province. Enhanced burning, in concert with abruptly altered precipitation and land-surface temperature regimes, likely contributed to vegetation dieback and the inhibition of seedling recruitment. Modern analogues in changing fire regimes indicate that increased fire frequency may have played a decisive role in the collapse of continental ecosystems during the EPE, even those populated by fire-tolerant wetland plants (Fig. 14). In addition to direct ecological stress for life on land, fires would have served as a positive feedback mechanism for greenhouse gas-driven warming, and a nutrient vector that catalyzed toxic microbial blooms in regional aquatic ecosystems.

Following the EPE, the micro- and mesofossil records confirm a 'charcoal depression' for at least the first three million years of the Early Triassic. The open vegetation of the Early Triassic had low biomass and was not conducive to extensive burning, despite initial atmospheric oxygen levels equal to or higher than today. Reduced drawdown of CO_2 (owing to reduced burial of terrestrial organic matter) in the Early Triassic likely contributed to prolonged greenhouse conditions until at least the Spathian Stage (c. 249 Ma). Fire returned as a major environmental process only with the re-establishment of complex forest ecosystems in the Middle Triassic.

FIG. 14.—Artist's reconstruction of the humid temperate but fire-adapted glossopterid biome during the end-Permian extinction interval (c. 252.1 Ma). Note the vegetative regeneration along the scorched trunks of the canopy-forming *Glossopteris*, but increased fire frequency during the EPE may have reduced the effectiveness of this fire-adapted strategy. Trackways of small therapsids, such as *Lystrosaurus* (Lystrosauridae; right), have been found in the Sydney Basin strata that correspond to this extinction interval (Harper 1915; Retallack 1996); this genus is one of the very few dicynodontid groups that survived the EPE. Artist: Victor O. Leshyk.

ACKNOWLEDGMENTS

We thank Jane Sibbons and Lucy McGee (University of Adelaide) for assistance with reflected light microscopy, Bob Hill (University of Adelaide) for discussions and sample logistics, Joan Esterle (University of Queensland) for advice on organic petrology. The authors acknowledge the support of research grant EAR-1636625 from the National Science Foundation, and the Swedish Research Council (VR) grant 2018-04527 to SM. The Australian Antarctic Division provided financial and logistical support for fieldwork in the Prince Charles Mountains during the Austral summer of 1994–1995 via Antarctic Science Advisory Council Project 509. We thank Editors Patrick John Orr, Will Foster, Kathleen Huber and Neil Davies, and reviewers Evelyn Kustatscher and André Jasper, for their constructive feedback.

SUPPLEMENTAL MATERIAL

Data are available from the PALAIOS Data Archive: https://www.sepm.org/supplemental-materials.

REFERENCES

ABU HAMAD, A.M.B., JASPER, A., AND UHL, D., 2012, The record of Triassic charcoal and other evidence for palaeo-wildfires: signal for atmospheric oxygen levels, taphonomic biases or lack of fuel?: International Journal of Coal Geology, v. 96–97, p. 60–71.

ALEXANDRIDIS, A., VAKALIS, D., SIETTOS, C.I., AND BAFAS, G.V., 2008, A cellular automata model for forest fire spread prediction: the case of the wildfire that swept through Spetses Island in 1990: Applied Mathematics and Computation, v. 204, p. 191–201.

ARRHENIUS, S., 1896, On the influence of carbonic acid in the air upon the temperature on the ground: Philosophical Magazine Series 5, v. 41, p. 237–275.

AYAZ, S.A., AMELIN, Y., NICOLL, R.S., ESTERLE, J.S., AND MARTIN, M.A., 2016a, Age of the Yarrabee and accessory tuffs: implications for the upper Permian sediment-accumulation rates across the Bowen Basin: Australian Journal of Earth Sciences, v. 63, p. 843–856.

AYAZ, S.A., RODRIGUES, S., GOLDING, S.D., AND ESTERLE, J.S., 2016b, Compositional variation and palaeoenvironment of the volcanolithic Fort Cooper Coal Measures, Bowen Basin, Australia: International Journal of Coal Geology, v. 166, p. 36–46.

BAKER, S.J., 2022, Fossil evidence that increased wildfire activity occurs in tandem with periods of global warming in Earth's past: Earth-Science Reviews, article 103871, doi: 10.1016/j.earscirev.2021.103871.

BAMBERRY, W.J., 1991, Stratigraphy and sedimentology of the late Permian Illawarra Coal Measures, southern Sydney Basin, New South Wales: Unpublished Ph.D.dissertation, University of Wollongong, Wollongong, 500 p.

BARRETT, K., BAXTER, R., KUKAVSKAYA, E., BALZTER, H., SHVETSOV, E., AND BURYAK, L., 2020, Postfire recruitment failure in Scots pine forests of southern Siberia: Remote Sensing of Environment, v. 237, article 111539, doi: 10.1016/j.rse.2019.111539.

BATTEN, D.J., 1996, Palynofacies and palaeoenvironmental interpretation, *in* J. Jansonius and D.C. McGregor (eds.), Palynology: Principles and Applications: American Association of Stratigraphic Palynologists Foundation, Los Angeles, p. 1011–1064.

BATTEN, D.J., 1998, Palaeoenvironmental implications of plant, insect and other organic-walled microfossils in the Weald Clay Formation (Lower Cretaceous) of southeast England: Cretaceous Research, v. 19, p. 279–315.

BECKMANN, M., VÁCLAVÍK, T., MANCEUR, A.M., ŠPRTOVÁ, L., VON WEHRDEN, H., WELK, E., AND CORD, A.F., 2014, glUV: a global UV-B radiation data set for macroecological studies: Methods in Ecology and Evolution, v. 5, p. 372–383, doi: 10.1111/2041-210X.12168.

BEERLING, D.J., HARFOOT, M., LOMAX, B., AND PYLE, J.A., 2007, The stability of the stratospheric ozone layer during the end-Permian eruption of the Siberian Traps: Philosophical Transactions of the Royal Society A, v. 365, p. 1843–1866, doi: 10.1098/rsta.2007.2046.

BELCHER, C.M. AND MCELWAIN, J.C., 2008, Limits for combustion in low O_2 redefine paleoatmospheric predictions for the Mesozoic: Science, v. 321, p. 1197–1200.

BELCHER, C.M., YEARSLEY, J.M., HADDEN, R.M., MCELWAIN, J.C., AND REIN, G., 2010, Baseline intrinsic flammability of Earth's ecosystems estimated from paleoatmospheric oxygen over the past 350 million years: Proceedings of the National Academy of Sciences of the United States of America, v. 107, p. 22448–22453.

BENCA, J.P., DUIJNSTEE, I.A.P., AND LOOY, C.V., 2018, UV-B–induced forest sterility: implications of ozone shield failure in Earth's largest extinction: Science Advances, v. 4, article e1700618, doi: 10.1126/sciadv.1700618.

Benda, L., Miller, D., Bigelow, P., and Andras, K., 2003, Effects of post-wildfire erosion on channel environments, Boise River, Idaho: Forest Ecology and Management, v. 178, p. 105–119, doi: 10.1016/S0378-1127(03)00056-2.

Benicio, J.R.W., Jasper, A., Spiekermann, R., Garavaglia, L., Pires-Oliveira, E.F., Machado, N.T.G., and Uhl, D., 2019, Recurrent palaeo-wildfires in a Cisuralian coal seam: a palaeobotanical view on high inertinite coals from the Lower Permian of the Paraná Basin, Brazil: PLOS One, v. 14, e0213854, doi: 10.1371/journal.pone.0213854.

Benton, M.J. and Newell, A.J., 2014, Impacts of global warming on Permo–Triassic terrestrial ecosystems: Gondwana Research, v. 25, p. 1308–1337.

Bergman, N.M., Lenton, T.M., and Watson, A.J., 2004, COPSE: a new model of biogeochemical cycling over Phanerozoic time: American Journal of Science, v. 304, p. 397–437.

Bernardi, M., Petti, F.M., and Benton, M.J., 2018, Tetrapod distribution and temperature rise during the Permian–Triassic mass extinction: Proceedings of the Royal Society B, v. 285, article 20172331, doi: 10.1098/rspb.2017.2331.

Berner, R.A., 2005, The carbon and sulfur cycles and atmospheric oxygen from middle Permian to middle Triassic: Geochimica et Cosmochimica Acta, v. 69, p. 3211–3217.

Berner, R.A., 2006, Carbon, sulfur and O_2 across the Permian–Triassic boundary: Journal of Geochemical Exploration, v. 88, p. 416–418.

Berner, R.A., 2009, Phanerozoic atmospheric oxygen: new results using the GEOCARBSULF model: American Journal of Science, v. 309, p. 603–606.

Bird, M.I., Wynn, J.G., Saiz, G., Wurster, C.M., and McBeath, A., 2015, The pyrogenic carbon cycle: Annual Review of Earth and Planetary Sciences, v. 43, p. 273–298.

Biswas, R.K., Kaiho, K., Saito, R., Tian, L., and Shi, Z., 2020, Terrestrial ecosystem collapse and soil erosion before the end-Permian marine extinction: organic geochemical evidence from marine and non-marine records: Global and Planetary Change, v. 195, article 103327, doi: 10.1016/j.gloplacha.2020.103327.

Black, B.A., Lamarque, J.-F., Shields, C.A., Elkins-Tanton, L.T., and Kiehl, J.T., 2014, Acid rain and ozone depletion from pulsed Siberian Traps magmatism: Geology, v. 42, p. 67–70, doi: https://doi.org/10.1130/G34875.1.

Black, B.A., Neely, R.R., Lamarque, J.-F., Elkins-Tanton, L.T., Kiehl, J.T., Shields, C.A., Mills, M.J., and Bardeen, C., 2018, Systemic swings in end-Permian climate from Siberian Traps carbon and sulfur outgassing: Nature Geoscience, v. 11, p. 949–954.

Bond, D.P.G. and Grasby, S.E., 2017, On the causes of mass extinctions: Palaeogeography, Palaeoclimatology, Palaeoecology, v. 478, p. 3–29.

Bordy, E.M. and Krummeck, W.D., 2016, Enigmatic continental burrows from the Early Triassic transition of the Katberg and Burgersdorp formations in the main Karoo Basin, South Africa: PALAIOS, v. 31, p. 389–403, doi: 10.2110/palo.2016.021.

Bordy, E.M., Sztanó, O., Rubidge, B.S., and Bumby, A., 2011, Early Triassic vertebrate burrows from the Katberg Formation of the south-western Karoo Basin, South Africa: Lethaia, v. 44, p. 33–45, doi: 10.1111/j.1502-3931.2010.00223.x.

Botha, J., Huttenlocker, A.K., Smith, R.M.H., Prevec, R., Viglietti, P., and Modesto, S.P., 2020, New geochemical and palaeontological data from the Permian–Triassic boundary in the South African Karoo Basin test the synchronocity of terrestrial and marine extinctions: Palaeogeography, Palaeoclimatology, Palaeoecology, v. 540, article 109467.

Botha-Brink, J., 2017, Burrowing in *Lystrosaurus*: preadaptation to a postextinction environment?: Journal of Vertebrate Paleontology, v. 37, e1365080, doi: 10.1080/02724634.2017.1365080.

Braadbaart, F. and Poole, I., 2008, Morphological, chemical and physical changes during charcoalification of wood and its relevance to archaeological contexts: Journal of Archaeological Science, v. 35, p. 2434–2445.

Brand, U., Davis, A.M., Shaver, K.K., Blamey, N.J.F., Heizler, M., and Lécuyer, C., 2021, Atmospheric oxygen of the Paleozoic: Earth-Science Reviews, v. 216, article 103560.

Brando, P.M., Balch, J.K., Nepstad, D.C., Morton, D.C., Putz, F.E., Coe, M.T., Silvério, D., Macedo, M.N., Davidson, E.A., Nóbreg, C.C., Alencar, A., and Soares-Filho, B.S., 2014, Abrupt increases in Amazonian tree mortality due to drought–fire interactions: Proceedings of the National Academy of Sciences of the United States of America, v. 111, p. 6347–6352.

Brando, P.M., Paolucci, L., Ummenhofer, C.C., Ordway, E.M., Hartmann, H., Cattau, M.E., Rattis, L., Medjibe, V., Coe, M.T., and Balch, J.K., 2019, Droughts, wildfires, and forest carbon cycling: a pantropical synthesis: Annual Review of Earth and Planetary Sciences, v. 47, p. 555–581, doi: 10.1146/annurev-earth-082517-010235.

Brtnicky, M., Datta, R., Holatko, J., Bielska, L., Gusiatin, Z.M., Kucerik, J., Hammerschmiedt, T., Danish, S., Radziemska, M., Mravcova, L., Fahad, S., Kintl, A., Sudoma, M., Ahmed, N., and Pecina, V., 2021, A critical review of the possible adverse effects of biochar in the soil environment: Science of the Total Environment, v. 796, article 148756, doi: 10.1016/j.scitotenv.2021.148756.

Burgess, S.D., Bowring, S., and Shen, S.-z. 2014, High-precision timeline for Earth's most severe extinction: Proceedings of the National Academy of Sciences of the United States of America, v. 111, p. 3316–3321.

Burgess, S.D., Muirhead, J.D., and Bowring, S.A., 2017, Initial pulse of Siberian Traps sills as the trigger of the end-Permian mass extinction: Nature Communications, v. 8, article 164, doi: 10.1038/s41467-017-00083-9.

Cai, Y.-F., Zhang, H., Cao, C.-Q., Zheng, Q.-F., Jin, C.-F., and Shen, S.-Z., 2021a, Wildfires and deforestation during the Permian–Triassic transition in the southern Junggar Basin, Northwest China: Earth-Science Reviews, v. 218, article 103670, doi: 10.1016/j.earscirev.2021.103670.

Cai, Y.-F., Zhang, H., Feng, Z., and Shen, S.-Z., 2021b, Intensive wildfire associated with volcanism promoted the vegetation changeover in southwest China during the Permian–Triassic transition: Frontiers in Earth Science, v. 9, article 615841, doi: 10.3389/feart.2021.615841.

Cantrill, D.J. and Webb, J.A., 1998, Permineralized pleuromeid lycopsid remains from the Early Triassic Arcadia Formation, Queensland, Australia: Review of Palaeobotany and Palynology, v. 102, p. 189–211.

Chen, J., Shen, S.-Z., Zhang, Y.-C., Angiolini, L., Nabi Gorgij, M., Crippa, G., Wang, W., Zhang, H., Yuan, D.-X., Li, X.-H., and Xu, Y.-G., 2020, Abrupt warming in the latest Permian detected using high-resolution in situ oxygen isotopes of conodont apatite from Abadeh, central Iran: Palaeogeography, Palaeoclimatology, Palaeoecology, v. 560, article 109973, doi: 10.1016/j.palaeo.2020.109973.

Chu, D., Dal Corso, J., Shu, W., Song, H., Wignall, P.B., Grasby, S.E., van de Schootbrugge, B., Zong, K., Wu, Y., and Tong, J., 2021, Metal-induced stress in survivor plants following the end-Permian collapse of land ecosystems: Geology, v. 49, p. 657–661, doi: 10.1130/G48333.1.

Chu, D., Grasby, S.E., Song, H., Dal Corso, J., Wang, Y., Mather, T.A., Wu, Y., Song, H., Shu, W., Tong, J., and Wignall, P.B., 2020, Ecological disturbance in tropical peatlands prior to marine Permian–Triassic mass extinction: Geology, v. 48, p. 288–292, doi: 10.1130/G46631.1.

Clark, J.S. and Patterson, W.A., 1997, Background and local charcoal in sediments: scales of fire evidence in the paleorecord, *in* J.S. Clark, H. Cachier, J.G. Goldammer, and B. Stocks (eds.), Sediment Records of Biomass Burning and Global Change: Springer, Berlin, p. 23–48.

Cope, M.J. and Chaloner, W.J., 1985, Wildfire, an interaction of biological and physical processes, *in* B. Tiffney (ed.), Geological Factors and the Evolution of Plants: Yale University Press, Hartford, p. 257–277.

Costa, B.M., Pantoja, D.L., Vianna, M.C.M., and Colli, G.R., 2013, Direct and short-term effects of fire on lizard assemblages from a neotropical savanna hotspot: Journal of Herpetology, v. 47, p. 502–510, doi: 10.1670/12-043.

Cury, R.T.D.S., Montibeller-Santos, C., Balch, J.K., Brando, P.M., and Torezan, J.M., 2020, Effects of fire frequency on seed sources and regeneration in southeastern Amazonia: Frontiers in Forests and Global Change, v. 3, article 82, doi: 10.3389/ffgc.2020.00082.

Dal Corso, J., Mills, B.J.W., Chu, D., Newton, R.J., Mather, T.A., Shu, W., Wu, Y., Tong, J., and Wignall, P.B., 2020, Permo–Triassic boundary carbon and mercury cycling linked to terrestrial ecosystem collapse: Nature Communications, v. 11, article 2962, doi: 10.1038/s41467-020-16725-4.

Dal Corso, J., Song, H., Callegaro, S., Chu, D., Sun, Y., Hilton, J., Grasby, S.E., Joachimski, M.M., and Wignall, P.B., 2022, Environmental crises at the Permian–Triassic mass extinction: Nature Reviews Earth and Environment, in press, doi: 10.1038/s43017-021-00259-4.

De Bano, L.F., 2000, The role of fire and soil heating on water repellency in wildland environments: a review: Journal of Hydrology, v. 231, p. 195–206, doi: 10.1016/S0022-1694(00)00194-3.

Decombeix, A.-L., Taylor, E.L., and Taylor, T.N., 2010, Epicormic shoots in a Permian gymnosperm from Antarctica: International Journal of Plant Sciences, v. 171, p. 772–782.

Decombeix, A.-L., Taylor, E.L., and Taylor, T.N., 2016, Bark anatomy of late Permian glossopterid trees from Antarctica: IAWA Journal, v. 37, p. 444–458.

Degani-Schmidt, I., Guerra-Sommer, M., de Oliveira Mendonça, J., Mendonça Filho, J.G., Jasper, A., Cazzulo-Klepzig, M., and Iannuzzi, R., 2015, Charcoalified logs as evidence of hypautochthonous/autochthonous wildfire events in a peat-forming environment from the Permian of southern Paraná Basin (Brazil): International Journal of Coal Geology, v. 146, p. 55–67.

Diessel, C.F.K., 2010, The stratigraphic distribution of inertinite: International Journal of Coal Geology, v. 81, p. 251–268.

Diessel, C.F.K. and Smyth, M., 1995, Petrographic constituents of Australian coals, *in* C.R. Ward, H.J. Harrington, C.W. Mallett, and J.W. Beeston (eds.), Geology of Australian Coal Basins: Geological Society of Australia, Coal Geology Group, Sydney, p. 63–81.

Dong, D., Yang, M., Wang, C., Wang, H., Li, Y., Luo, J., and Wu, W., 2013, Responses of methane emissions and rice yield to applications of biochar and straw in a paddy field: Journal of Soils and Sediments, v. 13, p. 1450–1460, doi: 10.1007/s11368-013-0732-0.

Dutta, P., 2002, Gondwana lithostratigraphy of Peninsular India: Gondwana Research, v. 5, p. 540–553.

Fairman, T.A., Nitschke, C.R., and Bennett, L.T., 2016, Too much, too soon? A review of the effects of increasing wildfire frequency on tree mortality and regeneration in temperate eucalypt forests: International Journal of Wildland Fire, v. 25, p. 831–848.

Feng, X., Merow, C., Liu, Z., Park, D.S., Roehrdanz, P.R., Maitner, B., Newman, E.A., Boyle, B.L., Lien, A., Burger, J.R., Pires, M.M., Brando, P.M., Bush, M.B., McMichael, C.N.H., Neves, D.M., Nikolopoulos, E.I., Saleska, S.R., Hannah, L., Breshears, D.D., Evans, T.P., Soto, J.R., Ernst, K.C., and Enquist, B.J., 2021, How deregulation, drought and increasing fire impact Amazonian biodiversity: Nature, v. 597, p. 516–521, doi: 10.1038/s41586-021-03876-7.

Feng, Z., Wei, H.-B., Guo, Y., He, X.-Y., Sui, Q., Zhou, Y., Liu, H.-Y., Gou, X.-D., and Lv, Y., 2020a, From rainforest to herbland: new insights into land plant responses to the end-Permian mass extinction: Earth-Science Reviews, v. 204, article 103153, doi: 10.1016/j.earscirev.2020.103153.

Feng, Z., Wei, H.-B., Ye, R.-H., Sui, Q., Gou, X.-D., Guo, Y., Liu, L.-J., and Yang, S.-L., 2020b, Latest Permian peltasperm plant from southwest China and its paleoenvironmental implications: Frontiers in Earth Science, v. 8, article 559430, doi: 10.3389/feart.2020.559430.

Fielding, C.R., Frank, T.D., Tevyaw, A.P., Savatic, K., Vajda, V., McLoughlin, S., Mays, C., Nicoll, R.S., Bocking, M., and Crowley, J.L., 2021, Sedimentology of the continental end-Permian extinction event in the Sydney Basin, eastern Australia: Sedimentology, v. 68, p. 30–62, doi: 10.1111/sed.12782.

Fielding, C.R., Frank, T.D., Vajda, V., McLoughlin, S., Mays, C., Tevyaw, A.P., Winguth, A., Winguth, C., Nicoll, R.S., Bocking, M., and Crowley, J.L., 2019, Age and pattern of the southern high-latitude continental end-Permian extinction constrained by multiproxy analysis: Nature Communications, v. 10, article 385, doi: 10.1038/s41467-018-07934-z.

Fielding, C.R. and Webb, J.A., 1995, Sedimentology of the Permian Radok Conglomerate in the Beaver Lake area of MacRobertson Land, East Antarctica: Geological Magazine, v. 132, p. 51–63.

Fielding, C.R. and Webb, J.A., 1996, Facies and cyclicity of the Late Permian Bainmedart Coal Measures in the northern Prince Charles Mountains, MacRobertson Land, Antarctica: Sedimentology, v. 43, p. 295–322.

Figueiral, I. and Willcox, G., 1999, Archaeobotany and sub-fossils: collecting and analytical techniques, *in* T.P. Jones and N.P. Rowe (eds.), Fossil Plants and Spores, Modern Techniques: Geological Society of London, p. 290–294.

Finkelstein, D.B., Pratt, L.M., and Brassell, S.C., 2006, Can biomass burning produce a globally significant carbon-isotope excursion in the sedimentary record?: Earth and Planetary Science Letters, v. 250, p. 501–510.

Fischer, B., Manzoni, S., Morillas, L., Garcia, M., Johnson, M., and Lyon, S., 2018, Improving agricultural water use efficiency with biochar—a synthesis of biochar effects on water storage and fluxes across scales: Science of the Total Environment, v. 657, p. 853–862, doi: 10.1016/j.scitotenv.2018.11.312.

Fleming, J.R., 1998, Historical Perspectives on Climate Change: Oxford University Press, Oxford, 194 p.

Florsheim, J.L., Keller, E.A., and Best, D.W., 1991, Fluvial sediment transport in response to moderate storm flows following chaparral wildfire, Ventura County, southern California: Geological Society of America Bulletin, v. 103, p. 504–511, doi: 10.1130/0016-7606(1991)103<0504:FSTIRT>2.3.CO;2.

Foster, C.B., 1982, Spore-pollen assemblages of the Bowen Basin, Queensland (Australia): their relationship to the Permian/Triassic boundary: Review of Palaeobotany and Palynology, v. 36, p. 165–183.

Foster, C.B. and Afonin, S.A., 2005, Abnormal pollen grains: an outcome of deteriorating atmospheric conditions around the Permian–Triassic boundary: Journal of the Geological Society of London, v. 162, p. 653–659.

Frank, T.D., Fielding, C.R., Winguth, A.M.E., Savatic, K., Tevyaw, A., Winguth, C., McLoughlin, S., Vajda, V., Mays, C., Nicoll, R., Bocking, M., and Crowley, J.L., 2021, Pace, magnitude, and nature of terrestrial climate change through the end Permian extinction in southeastern Gondwana: Geology, v. 49, p. 1089–1095, doi: 10.1130/G48795.1.

Gallagher, R.V., Allen, S., Mackenzie, B.D.E., Yates, C.J., Gosper, C.R., Keith, D.A., Merow, C., White, M.D., Wenk, E., Maitner, B.S., He, K., Adams, V.M., and Auld, T.D., 2021, High fire frequency and the impact of the 2019–2020 megafires on Australian plant diversity: Diversity and Distributions, v. 27, p. 1166–1179, doi: 10.1111/ddi.13265.

Galtier, J. and Phillips, T.L., 1999, The acetate peel technique, *in* T.P. Jones and N.P. Rowe (eds.), Fossil Plants and Spores: Modern Techniques: The Geological Society of London, p. 67–70.

Gastaldo, R.A., Kamo, S.L., Neveling, J., Geissman, J.W., Bamford, M., and Looy, C.V., 2015, Is the vertebrate-defined Permian–Triassic boundary in the Karoo Basin, South Africa, the terrestrial expression of the end-Permian marine event?: Geology, v. 43, p. 939–942, doi: 10.1130/G37040.1.

Gastaldo, R.A., Kus, K., Tabor, N., and Neveling, J., 2020, Calcic vertisols in the upper *Daptocephalus* Assemblage Zone, Balfour Formation, Karoo Basin, South Africa: implications for late Permian climate: Journal of Sedimentary Research, v. 90, p. 609–628.

Gastaldo, R.A. and Rolerson, M.W., 2008, *Katbergia* gen. nov., a new trace fossil from Upper Permian and Lower Triassic rocks of the Karoo Basin: implications for palaeoenvironmental conditions at the P/Tr extinction event: Palaeontology, v. 51, p. 215–229, doi: 10.1111/j.1475-4983.2007.00743.x.

Geary, W.L., Buchan, A., Allen, T., Attard, D., Bruce, M.J., Collins, L., Ecker, T.E., Fairman, T.A., Hollings, T., Loeffler, E., Muscatello, A., Parkes, D., Thomson, J., White, M., and Kelly, E., 2021, Responding to the biodiversity impacts of a megafire: a case study from south-eastern Australia's Black Summer: Diversity and Distributions, article 13292, doi: 10.1111/ddi.13292.

Gill, A.M., 1981, Fire adaptive traits of vascular plants, *in* H.A. Mooney, T.M. Bonnicksen, N.L. Christensen, J.E. Lotan, and W.A. Reiners (eds.), Fire Regimes and Ecosystem Properties: U.S. Forest Service Conference Proceedings, December 11–15, 1978, Honolulu, Hawaii, Washington, p. 208–230.

Glasspool, I., 2000, A major fire event recorded in the mesofossils and petrology of the Late Permian, Lower Whybrow coal seam, Sydney Basin, Australia: Palaeogeography, Palaeoclimatology, Palaeoecology, v. 164, p. 357–380, doi: 10.1016/S0031-0182(00)00194-2.

Glasspool, I.J. and Scott, A.C., 2010, Phanerozoic atmospheric oxygen concentrations reconstructed from sedimentary charcoal: Nature Geoscience, v. 3, p. 627–630, doi: 10.1038/NGEO923.

Glasspool, I.J. and Scott, A.C., 2013, Identifying past fire events, *in* C.M. Belcher (ed.), Fire Phenomena and the Earth System: An Interdisciplinary Guide to Fire Science: John Wiley and Sons, West Sussex, p. 179–206.

Glasspool, I.J., Scott, A.C., Waltham, D., Pronina, N., and Shao, L., 2015, The impact of fire on the late Paleozoic Earth system: Frontiers in Earth Science, v. 6, article 756, doi: 10.3389/fpls.2015.00756.

Goldammer, J.G. and Seibert, B., 1990, Tropical lowland rain forest of east Kalimantan, *in* J.G. Goldammer (ed.), The Impact of Droughts and Forest Fires: Springer-Verlag, Berlin, p. 11–31.

Goscombe, P.W., 1975, Nebo District, *in* D.M. Traves and D. King (eds.), Economic Geology of Australia and Papua New Guinea, 2, Coal: The Australasian Institute of Mining and Metallurgy, Parkville, p. 137–148.

Gould, R.E., 1970, *Palaeosmunda*, a new genus of siphonostelic osmundaceous trunks from the Upper Permian of Queensland: Palaeontology, v. 13, p. 10–28.

Gould, R.E., 1975, A preliminary report on petrified axes of *Vertebraria* from the Permian of eastern Australia, *in* K.S.W. Campbell (ed.), Gondwana Geology: Australian National University Press, Canberra, p. 109–115.

Gould, R.E. and Delevoryas, T., 1977, The biology of *Glossopteris*: evidence from petrified seed-bearing and pollen-bearing organs: Alcheringa, v. 1, p. 387–399.

Grasby, S.E., Liu, X., Yin, R., Ernst, R.E., and Chen, Z., 2020, Toxic mercury pulses into late Permian terrestrial and marine environments: Geology, v. 48, p. 830–833, doi: 10.1130/G47295.1.

Grice, K., Nabbefeld, B., and Maslen, E., 2007, Source and significance of selected polycyclic aromatic hydrocarbons in sediments (Hovea-3 well, Perth Basin, Western Australia) spanning the Permian–Triassic boundary: Organic Geochemistry, v. 38, p. 1795–1803.

Groenewald, G.H., Welman, J., and MacEachern, J.A., 2001, Vertebrate burrow complexes from the Early Triassic *Cynognathus* Zone (Driekoppen Formation, Beaufort Group) of the Karoo Basin, South Africa: PALAIOS, v. 16, p. 148–160, doi: 10.1669/0883-1351(2001)016,0148:VBCFTE.2.0.CO;2.

Gulbranson, E.L., Ryberg, P.E., Decombeix, A.-L., Taylor, E.L., Taylor, T.N., and Isbell, J.L., 2014, Leaf habit of Late Permian *Glossopteris* trees from high-palaeolatitude forests: Journal of the Geological Society of London, v. 171, p. 493–507, doi: 10.1144/jgs2013-127.

Harper, L.E., 1915, Geology and mineral resources of the southern coal-field: Geological Memoir of the Geological Survey of New South Wales, v. 7, p. 1–410.

Harrowfield, M., Holdgate, G., Wilson, C., and McLoughlin, S., 2005, Tectonic significance of the Lambert Graben, East Antarctica: reconstructing the Gondwanan rift: Geology, v. 33, p. 197–200.

Hass, H. and Rowe, N.P., 1999, Thin sections and wafering, *in* T.P. Jones and N.P. Rowe (eds.), Fossil Plants and Spores: Modern Techniques: The Geological Society of London, p. 76–81.

He, T., Belcher, C.M., Lamont, B.B., and Lim, S.L., 2016, A 350-million-year legacy of fire adaptation among conifers: Journal of Ecology, v. 104, p. 352–363, doi: 10.1111/1365-2745.12513.

Highton, P.J.C., Pearson, A., and Scott, A.C., 1991, Palynofacies and palynodebris and their use in Coal Measure palaeoecology and palaeoenvironmental analysis: Neues Jahrbuch für Geologie und Paläontologie-Abhandlungen, v. 183, p. 135–169.

Holdgate, G.R., McLoughlin, S., Drinnan, A.N., Finkelman, R.B., Willett, J.C., and Chiehowsky, L.A., 2005, Inorganic chemistry, petrography and palaeobotany of Permian coals in the Prince Charles Mountains, East Antarctica: International Journal of Coal Geology, v. 63, p. 156–177.

Holmes, W.B.K. and Anderson, H.M., 2013, A synthesis of the rich Gondwana Triassic megafossil flora from Nymboida, Australia, *in* L.H. Tanner, J.A. Spielmann, and S.G. Lucas (eds.), The Triassic System: New Mexico Museum of Natural History, Bulletin 61, Albuquerque, p. 296–305.

Hower, J.C., O'Keefe, J.M.K., Eble, C.F., Raymond, A., Valentim, B., Volk, T.J., Richardson, A.R., Satterwhite, A.B., Hatch, R.S., Stucker, J.D., and Watt, M.A., 2011, Notes on the origin of inertinite macerals in coal: evidence for fungal and arthropod transformations of degraded macerals: International Journal of Coal Geology, v. 86, p. 231–240.

Hudspith, V.A. and Belcher, C.M., 2017, Observations of the structural changes that occur during charcoalification: implications for identifying charcoal in the fossil record: Palaeontology, v. 60, p. 503–510.

Huleatt, M.B., 1991, Handbook of Australian Black Coals: Geology, Resources, Seam Properties, and Product Specifications: Australian Government Publishing Service, Canberra, 116 p.

Hunt, J.W., 1982, Relationship between microlithotype and maceral composition of coals and geological setting of coal measures in the Permian Basins of eastern Australia: Australian Coal Geology, v. 4, p. 484–502.

Hunt, J.W., 1989, Permian coals of eastern Australia: geological control of petrographic variation: International Journal of Coal Geology, v. 12, p. 589–634.

Hutton, L.J., Grimes, K.G., Law, S.R., and McLennan, T.P.T., 1991, Geology of the Mount Coolon 1:250 000 Sheet area: Geoscience Australia, Canberra, p. 1–113.

Huyskens, M.H., 2014, Improving precision and accuracy of U-Pb geochronology with application to the Permian period: Unpublished Ph.D. dissertation, Australian National University, Canberra, 136 p.

International Committee for Coal and Organic Petrology (ICCP), 2001, The new inertinite classification (ICCP System 1994): Fuel, v. 80, p. 459–471.

Jasper, A., Agnihotri, D., Tewari, R., Spiekermann, R., Fabbrin Pires, E., Rosa, Á.A.S.D., and Uhl, D., 2017, Fires in the mire: repeated fire events in Early Permian 'peat forming' vegetation of India: Geological Journal, v. 52, p. 955–969, doi: 10.1002/gj.2860.

Jasper, A., Guerra-Sommer, M., Abu Hamad, A.M.B., Bamford, M., Cerruti Bernardes-de-Oliveira, M.E., Tewari, R., and Uhl, D., 2013, The burning of Gondwana: Permian fires on the southern continent—a palaeobotanical approach: Gondwana Research, v. 24, p. 148–160.

Jasper, A., Guerra-Sommer, M., Uhl, D., Bernardes-de-Oliveira, M.E.C., Ghosh, A.K., Tewari, R., and Secchi, M.I., 2012, Palaeobotanical evidence of wildfire in the Upper Permian of India: macroscopic charcoal remains from the Raniganj Formation, Damodar Basin: The Palaeobotanist, v. 61, p. 75–82.

Jasper, A., Uhl, D., Agnihotri, D., Tewari, R., Pandita, S.K., Wanderley Benicio, J.R., Pires, E.F., Stock Da Rosa, Á.A., Bhat, G.D., and Pillai, S.S.K., 2016a, Evidence of wildfires in the Late Permian (Changsinghian) Zewan Formation of Kashmir, India: Current Science, v. 110, p. 419–423.

Jasper, A., Uhl, D., Tewari, R., Guerra-Sommer, M., Spiekermann, R., Manfroi, J., Osterkamp, I.C., Wanderley Benício, J.R., Cerruti Bernardes-de-Oliveira, M.E., Pires, E.F., and Stock da Rosa, Á.A., 2016b, Indo-Brazilian Late Palaeozoic wildfires: an overview on macroscopic charcoal: Geologia Universidade de São Paulo Série Cientifica, v. 16, p. 87–97.

Jefferson, T.H. and Taylor, T.N., 1983, Permian and Triassic woods from the Transantarctic Mountains: paleoenvironmental indicators: Antarctic Journal of the United States, v. 18, p. 55–57.

Jeffery, S., Verheijen, F.G.A., van der Velde, M., and Bastos, A.C., 2011, A quantitative review of the effects of biochar application to soils on crop productivity using meta-analysis: Agriculture, Ecosystems and Environment, v. 144, p. 175–187, doi: 10.1016/j.agee.2011.08.015.

Jessop, K., Daczko, N.R., and Piazolo, S., 2019, Tectonic cycles of the New England Orogen, eastern Australia: a review: Australian Journal of Earth Sciences, v. 66, p. 459–496, doi: 10.1080/08120099.2018.1548378.

Johnson, B., 1984, The great fire of Borneo: report of a visit to Kalimantan Timur a year later: World Wildlife Fund, Godalming, 22 p.

Jolly, W.M., Cochrane, M.A., Freeborn, P.H., Holden, Z.A., Brown, T.J., Williamson, G.J., and Bowman, D.M.J.S., 2015, Climate-induced variations in global wildfire danger from 1979 to 2013: Nature Communications, v. 6, article 7537, doi: 10.1038/ncomms8537.

Jones, J.G., Conaghan, P.J., and McDonnell, K.L., 1987, Coal measures of an orogenic recess: Late Permian Sydney Basin, Australia: Palaeogeography, Palaeoclimatology, Palaeoecology, v. 58, p. 203–219.

Jones, J.G., Conaghan, P.J., McDonnell, K.L., Flood, R.H., Shaw, S.E., 1984, Papuan Basin analogue and a foreland basin model for the Bowen-Sydney Basin, *in* J.J. Veevers (ed.), Phanerozoic Earth History of Australia: Clarendon Press, Oxford, p. 243–261.

Jones, T.P. and Chaloner, W.G., 1991, Fossil charcoal, its recognition and palaeoatmospheric significance: Palaeogeography Palaeoclimatology Palaeoecology, v. 97, p. 39–50.

Kaiho, K., Aftabuzzaman, M., Jones, D.S., and Tian, L., 2021, Pulsed volcanic combustion events coincident with the end-Permian terrestrial disturbance and the following global crisis: Geology, v. 49, p. 289–293, doi: 10.1130/G48022.1.

Kaiho, K., Oshima, N., Adachi, K., Adachi, Y., Mizukami, T., Fujibayashi, M., and Saito, R., 2016, Global climate change driven by soot at the K-Pg boundary as the cause of the mass extinction: Scientific Reports, v. 6, article 28427.

Kauffmann, M., Jasper, A., Uhl, D., Meneghini, J., Osterkamp, I.C., Zvirtes, G., and Fabbrin Pires, E. 2016, Evidence for palaeo-wildfire inthe Late Permian palaeotropics—charcoal from the Motuca Formation in the Parnaíba Basin, Brazil: Palaeogeography, Palaeoclimatology, Palaeoecology, v. 450, p. 122–128.

Keeley, J.E., Pausas, J.G., Rundel, P.W., Bond, W.J., and Bradstock, R.A., 2011, Fire as an evolutionary pressure shaping plant traits: Trends in Plant Science, v. 16, p. 406–411.

Kelly, L.T., Giljohann, K.M., Duane, A., Aquilué, N., Archibald, S., Batllori, E., Bennett, A.F., Buckland, S.T., Canelles, Q., Clarke, M.F., Fortin, M.-J., Hermoso, V., Herrando, S., Keane, R.E., Lake, F.K., McCarthy, M.A., Morán-Ordóñez, A., Parr, C.L., Pausas, J.G., Penman, T.D., Regos, A., Rumpff, L., Santos, J.L., Smith, A.L., Syphard, A.D., Tingley, M.W., and Brotons, L., 2020, Fire and biodiversity in the Anthropocene: Science, v. 370, eabb0355, doi: 10.1126/science.abb0355.

Klootwijk, C., 2016, Paleomagnetism of the Carboniferous Rouchel Block, Tamworth Belt, and pole path revision for the New England Orogen, eastern Australia: Australian Journal of Earth Sciences, v. 63, p. 513–549, doi: 10.1080/08120099.2016.1223170.

Krause, A.J., Mills, B.J.W., Zhang, S., Planavsky, N.J., Lenton, T.M., and Poulton, S.W., 2018, Stepwise oxygenation of the Paleozoic atmosphere: Nature Communications, v. 9, article 4081, doi: 10.1038/s41467-018-06383-y.

Kruger, F.J., 1983, Plant community diversity and dynamics in relation to fire, *in* F.J. Kruger, D.T. Mitchell, and J.U.M. Jarvis (eds.), Mediterranean-Type Ecosystems. Ecological Studies (Analysis and Synthesis): Springer, Berlin, p. 446–472.

Kurtz, A.C., Kump, L.R., Arthur, M.A., Zachos, J.C., and Paytan, A., 2003, Early Cenozoic decoupling of the global carbon and sulfur cycles: Paleoceanography and Paleoclimatology, v. 18, article 1090, doi: 10.1029/2003PA000908.

Kustatscher, E., van Konijnenburg-van Cittert, J.H.A., Looy, C.V., Labandeira, C.C., Wappler, T., Butzmann, R., Fischer, T.C., Krings, M., Kerp, H., and Visscher, H., 2017, The Lopingian (late Permian) flora from the Bletterbach Gorge in the Dolomites, Northern Italy: a review: Geo.Alp, v. 14, p. 39–61.

Laurie, J.R., Bodorkos, S., Nicoll, R.S., Crowley, J.L., Mantle, D.J., Mory, A.J., Wood, G.R., Backhouse, J., Holmes, E.K., Smith, T.E., and Champion, D.C., 2016, Calibrating the middle and late Permian palynostratigraphy of Australia to the geologic time-scale via U-Pb zircon CA-IDTIMS dating: Australian Journal of Earth Sciences, v. 63, p. 701–730.

Lehmann, J., Gaunt, J., and Rondon, M., 2006, Bio-char sequestration in terrestrial ecosystems—a review: Mitigation and Adaptation Strategies for Global Change, v. 11, p. 403–427, doi: 10.1007/s11027-005-9006-5.

Lenton, T.M., Daines, S.J., and Mills, B.J.W., 2018, COPSE reloaded: an improved model of biogeochemical cycling over Phanerozoic time: Earth-Science Reviews, v. 178, p. 1–28.

Lewis, D., 2020, 'Deathly silent': ecologist describes Australian wildfires' devastating aftermath: Nature, v. 577, article 304, doi: 10.1038/d41586-020-00043-2.

Lindström, S. and McLoughlin, S., 2007, Synchronous palynofloristic extinction and recovery after the end-Permian event in the Prince Charles Mountains, Antarctica: implications for palynofloristic turnover across Gondwana: Review of Palaeobotany and Palynology, v. 145, p. 89–122.

Lindström, S., McLoughlin, S., and Drinnan, A.N., 1997, Intraspecific variation of taeniate bisaccate pollen within Permian glossopterid sporangia, from the Prince Charles Mountains, Antarctica: International Journal of Plant Sciences, v. 158, p. 673–684.

Mahesh, S., Murthy, S., Chakraborty, B., and Roy, M.D., 2015, Fossil charcoal as palaeofire indicators: taphonomy and morphology of charcoal remains in sub-surface Gondwana sediments of South Karanpura Coalfield: Journal Geological Society of India, v. 85, p. 567–576.

Marengo, J.A., Cunha, A.P., Cuartas, L.A., Deusdará Leal, K.R., Broedel, E., Seluchi, M.E., Michelin, C.M., De Praga Baião, C.F., Chuchón Ângulo, E., Almeida, E.K., Kazmierczak, M.L., Antônio Mateus, N.P., Silva, R.C., and Bender, F., 2021, Extreme drought in the Brazilian Pantanal in 2019–2020: characterization, causes, and impacts: Frontiers in Water, v. 3, article 639204, doi: 10.3389/frwa.2021.639204.

Marod, D., Kutintara, U., Tanaka, H., and Nakashizuka, T., 2002, The effects of drought and fire on seed and seedling dynamics in a tropical seasonal forest in Thailand: Plant Ecology, v. 161, p. 41–57, doi: 10.1023/A:1020372401313.

Mays, C., Cantrill, D.J., and Bevitt, J.J., 2017, Polar wildfires and conifer serotiny during the Cretaceous global hothouse: Geology, v. 45, p. 1119–1122, doi: 10.1130/G39453.1.

Mays, C., McLoughlin, S., Frank, T.D., Fielding, C.R., Slater, S.M., and Vajda, V., 2021a, Lethal microbial blooms delayed freshwater ecosystem recovery following the end-Permian extinction: Nature Communications, v. 12, article 5511, doi: 10.1038/s41467-021-25711-3.

Mays, C., Vajda, V., Frank, T.D., Fielding, C.R., Nicoll, R.S., Tevyaw, A.P., and McLoughlin, S., 2020, Refined Permian–Triassic floristic timeline reveals early collapse and delayed recovery of south polar terrestrial ecosystems: Geological Society of America Bulletin, v. 132, p. 1489–1513, doi: 10.1130/B35355.1.

Mays, C., Vajda, V., and McLoughlin, S., 2021b, Permian–Triassic non-marine algae of Gondwana—distributions, natural affinities and ecological implications: Earth-Science Reviews, v. 212, article 103382, doi: 10.1016/j.earscirev.2020.103382.

McLoughlin, S., 2001, The breakup history of Gondwana and its impact on pre-Cenozoic floristic provincialism: Australian Journal of Botany, v. 49, p. 271–300.

McLoughlin, S., 2011, *Glossopteris*: Insights into the architecture and relationships of an iconic Permian Gondwanan plant: Journal of the Botanical Society of Bengal, v. 65, p. 1–14.

McLoughlin, S., 2021, History of Life: Plants: Gymnosperms, *in* S. Elias and D. Alderton (eds.), Encyclopedia of Geology: Elsevier, Amsterdam, p. 476–500.

McLoughlin, S., Bomfleur, B., and Drinnan, A.N., 2018, *Pachytestopsis tayloriorum* gen. et sp. nov., an anatomically preserved glossopterid seed from the Lopingian of Queensland, Australia, *in* M. Krings, C.J. Harper, N.R. Cuneo,and G.W. Rothwell (eds.), Transformative Paleobotany: Papers to Commemorate the Life and Legacy of Thomas N. Taylor: Academic Press, Cambridge, p. 155–178.

McLoughlin, S. and Drinnan, A.N., 1996, Anatomically preserved *Noeggerathiopsis* leaves from east Antarctica: Review of Palaeobotany and Palynology, v. 92, p. 207–227.

McLoughlin, S. and Drinnan, A.N., 1997a, Revised stratigraphy of the Permian Bainmedart Coal Measures, northern Prince Charles Mountains, East Antarctica: Geological Magazine, v. 134, p. 335–353.

McLoughlin, S. and Drinnan, A.N., 1997b, Fluvial sedimentology and revised stratigraphy of the Triassic Flagstone Bench Formation, northern Prince Charles Mountains, East Antarctica: Geological Magazine, v. 134, p. 781–806.

McLoughlin, S., Drinnan, A.N., Slater, B.J., and Hilton, J., 2015, *Paurodendron stellatum*: a new Permian permineralized herbaceous lycopsid from the Prince Charles Mountains, Antarctica: Review of Palaeobotany and Palynology, v. 220, p. 1–15.

McLoughlin, S., Lindström, S., and Drinnan, A.N., 1997, Gondwanan floristic and sedimentological trends during the Permian–Triassic transition: new evidence from the Amery Group, northern Prince Charles Mountains, East Antarctica: Antarctic Science, v. 9, p. 281–298.

McLoughlin, S., Maksimenko, A., and Mays, C., 2019, A new high-paleolatitude late Permian permineralized peat flora from the Sydney Basin, Australia: International Journal of Plant Sciences, v. 180, p. 513–539, doi: 10.1086/702939.

McLoughlin, S., Mays, C., Vajda, V., Bocking, M., Frank, T.D., and Fielding, C.R., 2020, Dwelling in the dead zone—vertebrate burrows immediately succeeding the end-Permian extinction event in Australia: PALAIOS, v. 35, p. 342–357, doi: 10.2110/palo.2020.007.

McLoughlin, S., Nicoll, R.S., Crowley, J.L., Vajda, V., Mays, C., Fielding, C.R., Frank, T.D., Wheeler, A., and Bocking, M., 2021, Age and paleoenvironmental significance of the Frazer Beach Member—a new lithostratigraphic unit overlying the end-Permian extinction horizon in the Sydney Basin, Australia: Frontiers in Earth Science, v. 8, article 600976, doi: 10.3389/feart.2020.600976.

McLoughlin, S. and Prevec, R., 2021, The reproductive biology of glossopterid gymnosperms—a review: Review of Palaeobotany and Palynology, v. 295, article 104527, doi: 10.1016/j.revpalbo.2021.104527.

McMinn, A., 1985, Palynostratigraphy of the Middle Permian coal sequences of the Sydney Basin: Australian Journal of Earth Sciences, v. 32, p. 301–309.

McParland, L.C., Collinson, M.E., Scott, A.C., Steart, D.C., Grassineau, N.V., and Gibbons, S.J., 2007, Ferns and fires: experimental charring of ferns compared to wood and implications for paleobiology, paleoecology, coal petrology, and isotope geochemistry: PALAIOS, v. 22, p. 528–538, doi: 10.2110/palo.2005.p05-138r.

Metcalfe, I., Crowley, J.L., Nicoll, R.S., and Schmitz, M., 2015, High-precision U-Pb CA-TIMS calibration of Middle Permian to Lower Triassic sequences, mass extinction and extreme climate-change in eastern Australian Gondwana: Gondwana Research, v. 28, p. 61–81.

Meyer, G.A., Pierce, J.L., Wood, S.H., and Jull, A.J.T., 2001, Fire, storms, and erosional events in the Idaho batholith: Hydrological Processes, v. 15, p. 3025–3038, doi: 10.1002/hyp.389.

Mills, B.J.W., Donnadieu, Y., and Goddéris, Y., 2021, Spatial continuous integration of Phanerozoic global biogeochemistry and climate: Gondwana Research, v. 100, p. 73–86, doi: 10.1016/j.gr.2021.02.011.

Moroeng, O.M., Keartland, J.M., Roberts, R.J., and Wagner, N.J., 2018, Characterization of coal using electron spin resonance: implications for the formation of inertinite macerals in the Witbank Coalfield, South Africa: International Journal of Coal Science and Technology, v. 5, p. 385–398.

Muir, R.A., Bordy, E.M., and Prevec, R., 2015, Lower Cretaceous deposit reveals first evidence of a post-wildfire debris flow in the Kirkwood Formation, Algoa Basin, Eastern Cape, South Africa: Cretaceous Research, v. 56, p. 161–179, doi: 10.1016/j.cretres.2015.04.005.

Muttoni, G., Gaetani, M., Kent, D.V., Sciunnach, D., Angiolini, L., Berra, F., Garzanti, E., Mattei, M., and Zanchi, A., 2009, Opening of the Neo-Tethys Ocean and the Pangea B to Pangea A transformation during the Permian: Geoarabia, v. 14, p. 17–48.

Nabbefeld, B., Grice, K., Summons, R.E., Hays, L.E., and Cao, C., 2010, Significance of polycyclic aromatic hydrocarbons (PAHs) in Permian/Triassic boundary sections: Applied Geochemistry, v. 25, p. 1374–1382.

Neish, P.G., Drinnan, A.N., and Cantrill, D.J., 1993, Structure and ontogeny of *Vertebraria* from silicified Permian sediments in East Antarctica: Review of Palaeobotany and Palynology, v. 79, p. 221–244.

Nishida, H., Pigg, K.B., and De Vore, M.L., 2018, Glossopterid plant remains in permineralization: what do they tell us?, *in* M. Krings, C.J. Harper, N.R. Cúneo, and G.W. Rothwell (eds.), Transformative Paleobotany: Papers to Commemorate the Life and Legacy of Thomas N. Taylor: Elsevier, Amsterdam, p. 145–154.

Nishida, H., Pigg, K.B., Kudo, K., and Rigby, J.F., 2007, New evidence of reproductive organs of *Glossopteris* based on permineralized fossils from Queensland, Australia, I, ovulate organ *Homevaleia* gen. nov.: Journal of Plant Research, v. 120, p. 539–549.

Nishida, H., Pigg, K.B., Kudo, K., and Rigby, J.F., 2013, New evidence of the reproductive organs of *Glossopteris* based on permineralized fossils from Queensland, Australia, II: pollen-bearing organ E*diea* gen. nov.: Journal of Plant Research, v. 127, p. 233–240.

Nowack, J., Cooper, C.E., and Geiser, F., 2016, Cool echidnas survive the fire: Proceedings of the Royal Society B, v. 283, article 20160382, doi: 10.1098/rspb.2016.0382.

Oliver, C.F., 2011, An Investigation into the Degradation of Biochar and its Interactions with Plants and Soil Microbial Community: Unpublished M.Sc. Thesis, Stellenbosch University, Stellenbosch, 173 p.

Palansooriya, K.N., Wong, J.T.F., Hashimoto, Y., Huang, L., Rinklebe, J., Chang, S.X., Bolan, N., Wang, H., and Ok, Y.S., 2019, Response of microbial communities to biochar-amended soils: a critical review: Biochar, v. 1, p. 3–22, doi: 10.1007/s42773-019-00009-2.

Pausas, J.G., Bradstock, R.A., Keith, D.A., Keeley, J.E., and the Global Change of Terrestrial Ecosystems Fire Network, 2004, Plant functional traits in relation to fire in crown-fire ecosystems: Ecology, v. 85, p. 1085–1100.

Phillips, L.J., Crowley, J.L., Mantle, D.J., Esterle, J.S., Nicoll, R.S., McKellar, J.L., and Wheeler, A., 2018, U-Pb geochronology and palynology from Lopingian (upper Permian) coal measure strata of the Galilee Basin, Queensland, Australia: Australian Journal of Earth Sciences, v. 65, p. 153–173.

Pietikäinen, J., Kiikkilä, O., and Fritze, H., 2000, Charcoal as a habitat for microbes and its effect on the microbial community of the underlying humus: Oikos, v. 89, p. 231–242, doi: 10.1034/j.1600-0706.2000.890203.x.

Pigg, K.B. and McLoughlin, S., 1997, Anatomically preserved *Glossopteris* leaves from the Bowen and Sydney basins, Australia: Review of Palaeobotany and Palynology, v. 97, p. 339–359.

Pivello, V.R., Vieira, I., Christianini, A.V., Bandini Ribeiro, D., da Silva Menezes, L., Berlinck, C.N., Melo, F.P.L., Marengo, J.A., Tornquist, C.G., Moraes Tomas, W., and Overbeck, G.E., 2021, Understanding Brazil's catastrophic fires: causes, consequences and policy needed to prevent future tragedies: Perspectives in Ecology and Conservation, v. 19, p. 233–255.

Price, P.L., 1983, A Permian palynostratigraphy for Queensland, *in* C.G. Murray (ed.), Proceedings of the Symposium on the Permian Geology of Queensland: Geological Society of Australia, Queensland Division, Brisbane, p. 155–212.

Price, P.L., 1997, Permian to Jurassic palynostratigraphic nomenclature of the Bowen and Surat basins, *in* P.M. Green (ed.), The Surat and Bowen Basins, Southeast Queensland: Queensland Department of Mines and Energy, Brisbane, Australia, p. 137–178.

Putz, M.K. and Taylor, E.L., 1996, Wound response in fossil trees from Antarctica and its potential as a paleoenvironmental indicator: IAWA Journal, v. 17, p. 77–88.

Ranalli, A.J., 2004, A summary of the scientific literature on the effects of fire on the concentration of nutrients in surface waters: U.S. Geological Survey Open-File Report 2004-1296, U.S. Geological Survey, Reston, 23 p.

Recher, H.F., Lunney, D., and Matthews, A., 2009, Small mammal populations in a eucalypt forest affected by fire and drought, I, long-term patterns in an era of climate change: Wildlife Research, v. 36, p. 143–158, doi: 10.1071/WR08086.

Reichow, M.K., Pringle, M.S., Al'Mukhamedov, A.I., Allen, M.B., Andreichev, V.L., Buslov, M.M., Davies, C.E., Fedoseev, G.S., Fitton, J.G., Inger, S., Medvedev, A.Y., Mitchell, C., Puchkov, V.N., Safonova, I.Y., Scott, R.A., and Saunders, A.D., 2009, The timing and extent of the eruption of the Siberian Traps large igneous province: implications for the end-Permian environmental crisis: Earth and Planetary Science Letters, v. 277, p. 9–20.

Rengers, F.K., McGuire, L.A., Oakley, N.S., Kean, J.W., Staley, D.M., and Tang, H., 2017, Landslides after wildfire: initiation, magnitude, and mobility: Landslides, v. 17, p. 2631–2641, doi: 10.1007/s10346-020-01506-3.

Retallack, G.J., 1980, Late Carboniferous to Middle Triassic megafossil floras from the Sydney Basin, *in* R. Helby and C. Herbert (eds.), Geology of the Sydney Basin: Geological Survey of New South Wales, Sydney, p. 384–430.

Retallack, G.J., 1996, Early Triassic therapsid footprints from the Sydney Basin, Australia: Alcheringa, v. 20, p. 301–314, doi: 10.1080/03115519608619473.

Retallack, G.J., 1999, Post-apocalyptic greenhouse paleoclimate revealed by earliest Triassic paleosols in the Sydney Basin, Australia: Geological Society of America Bulletin, v. 111, p. 52–70.

Retallack, G.J., 2002, *Lepidopteris callipteroides*, an earliest Triassic seed fern of the Sydney Basin, southeastern Australia: Alcheringa, v. 26, p. 475–500.

Retallack, G.J., 2018, Leaf preservation in *Eucalyptus* woodland as a model for sclerophyll fossil floras: Alcheringa, v. 43, p. 71–84.

Retallack, G.J., Sheldon, N.D., Carr, P.F., Fanning, M., Thompson, C.A., Williams, M.L., Jones, B.G., and Hutton, A., 2011, Multiple Early Triassic greenhouse crises impeded recovery from Late Permian mass extinction: Palaeogeography Palaeoclimatology Palaeoecology, v. 308, p. 233–251.

Retallack, G.J., Veevers, J.J., and Morante, R., 1996, Global coal gap between Permian–Triassic extinction and Middle Triassic recovery of peat-forming plants: Geological Society of America Bulletin, v. 108, p. 195–207.

Richardson, A.R., Eble, C.F., Hower, J.C., and O'Keefe, J.M.K., 2012, A critical re-examination of the petrology of the No. 5 Block coal in eastern Kentucky with special attention to the origin of inertinite macerals in the splint lithotypes: International Journal of Coal Geology, v. 98, p. 41–49.

Rowe, E.R., D'Amato, A.W., Palik, B.J., and Almendinger, J.C., 2017, Early response of ground layer plant communities to wildfire and harvesting disturbance in forested peatland ecosystems in northern Minnesota, USA: Forest Ecology and Management, v. 398, p. 140–152, doi: 10.1016/j.foreco.2017.05.012.

Ryan, S.E., Dwyer, K.A., and Dixon, M.K., 2011, Impacts of wildfire on runoff and sediment loads at Little Granite Creek, western Wyoming: Geomorphology, v. 129, p. 113–130, doi: 10.1016/j.geomorph.2011.01.017.

Saito, M., 1990, Charcoal as a microhabitat for VA mycorrhizal fungi, and its practical applications: Agriculture, Ecosystems and Environment, v. 29, p. 341–344.

Sanei, H., Grasby, S.E., and Beauchamp, B., 2012, Latest Permian mercury anomalies Geology, v. 40, p. 63–66.

Scotese, C.R. and Langford, R.P., 1995, Pangea and the paleogeography of the Permian, *in* P.A. Scholle, T.M. Peryt, and D.S. Ulmer-Scholle (eds.), The Permian of Northern Pangea: Springer-Verlag, Berlin, p. 3–19.

Scott, A.C., 2000, The Pre-Quaternary history of fire: Palaeogeography, Palaeoclimatology, Palaeoecology, v. 164, p. 281–329.

Scott, A.C., 2010, Charcoal recognition, taphonomy and uses in palaeoenvironmental analysis: Palaeogeography, Palaeoclimatology, Palaeoecology, v. 291, p. 11–39, doi: 10.1016/j.palaeo.2009.12.012.

Scott, A.C., Cripps, J.A., Collinson, M.E., and Nichols, G.J., 2000, The taphonomy of charcoal following a recent heathland fire and some implications for the interpretation of

fossil charcoal deposits: Palaeogeography, Palaeoclimatology, Palaeoecology, v. 164, p. 1–31.

Scott, A.C. and Glasspool, I.J., 2006, The diversification of Paleozoic fire systems and fluctuations in atmospheric oxygen concentration: Proceedings of the National Academy of Sciences of the United States of America, v. 103, p. 10861–10865.

Scott, A.C. and Glasspool, I.J., 2007, Observations and experiments on the origin and formation of inertinite group macerals: International Journal of Coal Geology, v. 70, p. 53–66.

Scott, A.C. and Jones, T.P., 1991, Microscopical observations of recent and fossil charcoal: Microscopy and Analysis, v. 24, p. 13–15.

Scott, A.C. and Jones, T.P., 1994, The nature and influence of fire in Carboniferous ecosystems: Palaeogeography, Palaeoclimatology, Palaeoecology, v. 106, p. 91–112.

Seiler, W. and Crutzen, P.J., 1980, Estimates of gross and net fluxes of carbon between the biosphere and the atmosphere from biomass burning: Climatic Change, v. 2, p. 207–247.

Seneviratne, S.I., Zhang, X., Adnan, M., Badi, W., Dereczynski, C., Di Luca, A., Ghosh, S., Iskandar, I., Kossin, J., Lewis, S., Otto, F., Pinto, I., Satoh, M., Vicente-Serrano, S.M., Wehner, M., and Zhou, B., 2021, Weather and climate extreme events in a changing climate, *in* V. Masson-Delmotte, P. Zhai, A. Pirani, S.L. Connors, C. Péan, S. Berger, N. Caud, Y. Chen, L. Goldfarb, M.I. Gomis, M. Huang, K. Leitzell, E. Lonnoy, J.B.R. Matthews, T.K. Maycock, T. Waterfield, O. Yelekçi, R. Yu, and B. Zhou (eds.), Climate Change 2021: The Physical Science Basis. Contribution of Working Group I to the Sixth Assessment Report of the Intergovernmental Panel on Climate Change: Cambridge University Press, Cambridge, p. 345.

Sephton, M.A., Jiao, D., Engel, M.H., Looy, C.V., and Visscher, H., 2015, Terrestrial acidification during the end-Permian biosphere crisis?: Geology, v. 43, p. 159–162.

Shah, B.A., 2021, Diagenesis and genesis of clay minerals in the Triassic sandstones of the Panchet and Parsora formations, Damodar-Son Basin, India: Journal of Sedimentary Environments, v. 6, p. 255–265.

Shakesby, R.A. and Doerr, S.H., 2006, Wildfire as a hydrological and geomorphological agent: Earth-Science Reviews, v. 74, p. 269–307, doi: 10.1016/j.earscirev.2005.10.006.

Shen, J., Yu, J., Chen, J., Algeo, T.J., Xu, G., Feng, Q., Shi, X., Planavsky, N.J., Shu, W., and Xie, S., 2019, Mercury evidence of intense volcanic effects on land during the Permian–Triassic transition: Geology, v. 47, p. 1117–1121.

Shen, S.-Z., Crowley, J.L., Wang, Y., Bowring, S.A., Erwin, D.H., Sadler, P.M., Cao, C.-Q., Rothman, D.H., Henderson, C.M., Ramezani, J., Zhang, H., Shen, Y., Wang, X.-D., Wang, W., Mu, L., Li, W.-Z., Tang, Y.-G., Liu, X.-L., Liu, L.-J., Zeng, Y., Jiang, Y.-F., and Jin, Y.-G., 2011a, Calibrating the end-Permian mass extinction: Science, v. 334, p. 1367–1372.

Shen, W., Sun, Y., Lin, Y., Liu, D., and Chai, P., 2011b, Evidence for wildfire in the Meishan section and implications for Permian–Triassic events: Geochimica et Cosmochimica Acta, v. 75, p. 1992–2006.

Shi, G.R. and McLoughlin, S., 1997, Permian stratigraphy, sedimentology and palaeontology of the southern Sydney Basin, eastern Australia—a field excursion guide: Deakin University, School of Aquatic Science and Natural Resources Management, Melbourne, 59 p.

Shivanna, M., Murthy, S., Gautam, S., Souza, P.A., Kavali, P.S., Cerruti Bernardes-de-Oliveir, M.E., Ram-Awatar, Moreira Félix, C., 2017, Macroscopic charcoal remains as evidence of wildfire from late Permian Gondwana sediments of India: further contribution to global fossil charcoal database: Palaeoworld, v. 26, p. 638–649.

Sidor, C.A., Miller, M.F., and Isbell, J.L., 2008, Tetrapod burrows from the Triassic of Antarctica: Journal of Vertebrate Paleontology, v. 28, p. 277–284, doi: 10.1671/0272-4634(2008)28[277:TBFTTO]2.0.CO;2.

Slater, B.J., McLoughlin, S., and Hilton, J., 2011, Guadalupian (Middle Permian) megaspores from a permineralised peat in the Bainmedart Coal Measures, Prince Charles Mountains, Antarctica: Review of Palaeobotany and Palynology, v. 167, p. 140–155.

Slater, B.J., McLoughlin, S., and Hilton, J., 2012, Animal-plant interactions in a Middle Permian permineralised peat of the Bainmedart Coal Measures, Prince Charles Mountains, Antarctica: Palaeogeography Palaeoclimatology Palaeoecology, v. 363–364, p. 109–126.

Slater, B.J., McLoughlin, S., and Hilton, J., 2013, Peronosporomycetes (Oomycota) from Middle Permian permineralized peats of the Bainmedart Coal Measures, Prince Charles Mountains, Antarctica: PLOS One, v. 8, article e70707, doi: 10.1371/journal.pone.0070707.

Slater, B.J., McLoughlin, S., and Hilton, J., 2015, A high-latitude Gondwanan Lagerstätte: the Permian permineralised peat biota of the Prince Charles Mountains, Antarctica: Gondwana Research, v. 27, p. 1446–1473, doi: 10.1016/j.gr.2014.01.004.

Smith, H.G., Sheridan, G.J., Lane, P.N.J., Nyman, P., and Haydon, S., 2011, Wildfire effects on water quality in forest catchments: a review with implications for water supply: Journal of Hydrology, v. 396, p. 170–192.

Smith, R.M.H., Angielczyk, K.D., Benoit, J., and Fernandez, V., 2021, Neonate aggregation in the Permian dicynodont *Diictodon* (Therapsida, Anomodontia): evidence for a reproductive function for burrows?: Palaeogeography, Palaeoclimatology, Palaeoecology, v. 569, article 110311, doi: 10.1016/j.palaeo.2021.110311.

Smith, R.M.H. and Botha, J., 2005, The recovery of terrestrial vertebrate diversity in the South African Karoo Basin after the end-Permian extinction: Comptes Rendus Palevol, v. 4, p. 623–636, doi: 10.1016/j.crpv.2005.07.005.

Smith, R.M.H. and Botha-Brink, J., 2014, Anatomy of a mass extinction: sedimentological and taphonomic evidence for drought-induced die-offs at the Permo–Triassic boundary in the main Karoo Basin, South Africa: Palaeogeography, Palaeoclimatology, Palaeoecology, v. 396, p. 99–118.

Sobolev, S.V., Sobolev, A.V., Kuzmin, D.V., Krivolutskaya, N.A., Petrunin, A.G., Arndt, N.T., Radko, V.A., and Vasiliev, Y.R., 2011, Linking mantle plumes, large igneous provinces and environmental catastrophes: Nature, v. 477, p. 312–316, doi: 10.1038/nature10385.

Stach, E., 1982, The macerals of coal, *in* E. Stach, M.-T. Mackowsky, M. Teichmüller, G.H. Taylor, D. Chandra, and R. Teichmüller (eds.), Stach's Textbook of Coal Petrology: Gebrüder Borntraeger, Berlin, p. 87–138.

Stanley, S.M., 2016, Estimates of the magnitudes of major marine mass extinctions in earth history: Proceedings of the National Academy of Sciences, v. 113, p. e6325–e6334, doi: 10.1073/pnas.1613094113.

Sun, T., Guzman, J.J.L., Seward, J.D., Enders, A., Yavitt, J.B., Lehmann, J., Largus, T., and Angenent, L.T., 2021, Suppressing peatland methane production by electron snorkeling through pyrogenic carbon in controlled laboratory incubations: Nature Communications, v. 12, article 4119, doi: 10.1038/s41467-021-24350-y.

Sun, Y.D., Joachimski, M.M., Wignall, P.B., Yan, C.B., Chen, Y.L., Jiang, H.S., Wang, L.D., and Lai, X.L., 2012, Lethally hot temperatures during the Early Triassic Greenhouse: Science, v. 338, p. 366–370.

Svensen, H., Planke, S., Polozov, A.G., Schmidbauer, N., Corfu, F., Podladchikov, Y.Y., and Jamtveit, B., 2009, Siberian gas venting and the end-Permian environmental crisis: Earth and Planetary Science Letters, v. 277, p. 490–500.

Svensen, H.H., Frolov, S., Akhmanov, G.G., Polozov, A.G., Jerram, D.A., Shiganova, O.V., Melnikov, N.V., Iyer, K., and Planke, S., 2018, Sills and gas generation in the Siberian Traps: Philosophical Transactions of the Royal Society A, v. 376, article 20170080, doi: 10.1098/rsta.2017.0080.

Tan, D., Liu, Z., Jiang, L., Luo, J., and Li, J., 2017, Long-term potash application and wheat straw return reduced soil potassium fixation and affected crop yields in North China: Nutrient Cycling in Agroecosystems, v. 108, p. 121–133.

Tang, W., Llort, J., Weis, J., Perron, M.M.G., Basart, S., Li, Z., Sathyendranath, S., Jackson, T., Sanz Rodriguez, E., Proemse, B.C., Bowie, A.R., Schallenberg, C., Strutton, P.G., Matear, R., and Cassar, N., 2021, Widespread phytoplankton blooms triggered by 2019–2020 Australian wildfires: Nature, v. 597, p. 370–375, doi: 10.1038/s41586-021-03805-8.

Teichmüller, M. and Teichmüller, R., 1982, The geological basis of coal formation, *in* E. Stach, M.-T. Mackowsky, M. Teichmüller, G.H. Taylor, D. Chandra, and R. Teichmüller (eds.), Stach's Textbook of Coal Petrology: Gebrüder Borntraeger, Berlin, p. 5–86.

Tewari, R., Chatterjee, S., Agnihotri, D., and Pandita, S.K., 2015, *Glossopteris* flora in the Permian Weller formation of Allan Hills, South Victoria Land, Antarctica: implications for paleogeography, paleoclimatology, and biostratigraphic correlation: Gondwana Research, v. 28, p. 905–932, doi: 10.1016/j.gr.2015.02.003.

Tilston, E.L., Philippa, L., Ascough, P.L., Garnett, M.H., and Bird, M.I., 2016, Quantifying charcoal degradation and negative priming of soil organic matter with a ^{14}C-dead tracer: Radiocarbon, v. 58, p. 905–919, doi: 10.1017/RDC.2016.45.

Todd, C.N., Roberts, E.M., and Charles, A.J., 2021, A revised Permian–Triassic stratigraphic framework for the northeastern Galilee Basin, Queensland, Australia, and definition of a new Middle–Upper Triassic sedimentary unit: Australian Journal of Earth Sciences, v. 69, p. 113–134, doi: 10.1080/08120099.2021.1931962.

Tomas, W.M., Berlinck, C.N., Chiaravalloti, R.M., Paganini Faggioni, G., Strussmann, C., Libonati, R., Abrahão, C.R., do Valle Alvarenga, G., de Faria Bacellar, A.E., de Queiroz Batista, F.R., Silva Bornato, T., Restel Camilo, A., Castedo, J., Espinóza Fernando, A.M., Oliveira de Freitas, G., Martins Garcia, C., Santos Gonçalves, H., Butti de Freitas Guilherme, M., Guedes Layme, V.M., Gomes Lustosa, A.P., Carneiro de Oliveira, A., da Rosa Oliveira, M., de Matos Martins Pereira, A., Abrantes Rodrigues, J., Fernandes Semedo, T.B., Ducel de Souza, R.A., Tortato, F.R., Passos Viana, D.F., Vicente-Silva, L., and Morato, R., 2021, Counting the dead: 17 million vertebrates directly killed by the 2020's wildfires in the Pantanal wetland, Brazil: Scientific Reports, doi: 10.21203/rs.3.rs-859794/v1.

Torsvik, T.H., Van der Voo, R., Preeden, U., Mac Niocaill, C., Steinberger, B., Doubrovine, P.V., van Hinsbergen, D.J.J., Domeier, M., Gaina, C., Tohver, E., Meert, J.G., McCausland, P.J.A., and Cocks, L.R.M., 2012, Phanerozoic polar wander, palaeogeography and dynamics: Earth-Science Reviews, v. 114, p. 325–368.

Turner, M.G., Braziunas, K.H., Hansen, W.D., and Harvey, B.J., 2019, Short-interval severe fire erodes the resilience of subalpine lodgepole pine forests: Proceedings of the National Academy of Sciences of the United States of America, v. 116, p. 11319–11328.

Tyson, R.V., 1995, Sedimentary Organic Matter: Organic Facies and Palynofacies: Chapman and Hall, London, 615 p.

Uhl, D., Abu Hamad, A., Kerp, H., and Bandel, K., 2007, Evidence for palaeo-wildfire in the Late Permian palaeotropics—charcoalified wood from the Um Irna Formation of Jordan: Review of Palaeobotany and Palynology, v. 144, p. 221–230.

Uhl, D., Butzmann, R., Fischer, T.C., Meller, B., and Kustatscher, E., 2012, Wildfires in the late Palaeozoic and Mesozoic of the Southern Alps—the late Permian of the Bletterbach-Butterloch area (northern Italy): Rivista Italiana di Paleontologia e Stratigrafia, v. 118, p. 223–233.

Uhl, D., Jasper, A., Abu Hamad, A., and Montenari, M., 2008, Permian and Triassic wildfires and atmospheric oxygen levels, Proceedings of the 1st WSEAS International Conference on Environmental and Geological Science and Engineering (EG'08), p. 179–187.

Uhl, D., Jasper, A., Schindler, T., and Wuttke, M., 2010, Evidence of paleowildfire in the early Middle Triassic (early Anisian) *Voltzia* Sandstone: the oldest post-Permian macroscopic evidence of wildfire discovered so far: PALAIOS, v. 25, p. 837–842.

Uhl, D. and Kerp, H., 2003, Wildfires in the late Palaeozoic of Central Europe—the Zechstein (Upper Permian) of NW-Hesse (Germany): Palaeogeography, Palaeoclimatology, Palaeoecology, v. 199, p. 1–15.

Vajda, V., McLoughlin, S., Mays, C., Frank, T., Fielding, C.R., Tevyaw, A., Lehsten, V., Bocking, M., and Nicoll, R.S., 2020, End-Permian (252 Mya) deforestation, wildfires and flooding—an ancient biotic crisis with lessons for the present: Earth and Planetary Science Letters, v. 529, article 115875, doi: 10.1016/j.epsl.2019.115875.

van der Velde, I.R., van der Werf, G.R., Houweling, S., Maasakkers, J.D., Borsdorff, T., Landgraf, J., Tol, P., van Kempen, T.A., van Hees, R., Hoogeveen, R., Veefkind, J.P., and Aben, I., 2021, Vast CO_2 release from Australian fires in 2019–2020 constrained by satellite: Nature, v. 597, p. 366–369, doi: 10.1038/s41586-021-03712-y.

van der Werf, G.R., Randerson, J.T., Giglio, L., van Leeuwen, T.T., Chen, Y., Rogers, B.M., Mu, M., van Marle, M.J.E., Morton, D.C., Collatz, G.J., Yokelson, R.J., and Kasibhatla, P.S., 2017, Global fire emissions estimates during 1997–2016: Earth System Science Data, v. 9, p. 697–720, doi: 10.5194/essd-9-697-2017.

van Oldenborgh, G.J., Krikken, F., Lewis, S., Leach, N.J., Lehner, F., Saunders, K.R., van Weele, M., Haustein, K., Li, S., Wallom, D., Sparrow, S., Julie, A., Singh, R.P., van Aalst, M.K., Philip, S.Y., Vautard, R., and Otto, F.E.L., 2021, Attribution of the Australian bushfire risk to anthropogenic climate change: Natural Hazards and Earth System Sciences, v. 21, p. 941–960, doi: 10.5194/nhess-21-941-2021.

Veevers, J.J., 2006, Updated Gondwana (Permian–Cretaceous) earth history of Australia: Gondwana Research, v. 9, p. 231–260.

Veevers, J.J., Conaghan, P.J., and Shaw, S.E., 1994, Turning point in Pangean environmental history at the Permian/Triassic (P/Tr) boundary: Geological Society of America Special Paper, v. 288, p. 187–196.

Vieira, D.C.S., Fernández, C., Vega, J.A., and Keizer, J.J., 2015, Does soil burn severity affect the post-fire runoff and interrill erosion response? A review based on meta-analysis of field rainfall simulation data: Journal of Hydrology, v. 523, p. 452–464, doi: 10.1016/j.jhydrol.2015.01.071.

Visscher, H., Looy, C.V., Collinson, M.E., Brinkhuis, H., van Konijnenburg-van Cittert, J.H.A., Kürschner, W.M., and Sephton, M.A., 2004, Environmental mutagenesis during the end-Permian ecological crisis: Proceedings of the National Academy of Sciences of the United States of America, v. 101, p. 12952–12956, doi: 10.1073/pnas.0404472101.

Wan, M.-L., Yang, W., Wan, S., and Wang, J., 2021, Wildfires in the Early Triassic of northeastern Pangaea: evidence from fossil charcoal in the Bogda Mountains, northwestern China: Palaeoworld, v. 30, p. 593–601, doi: 10.1016/j.palwor.2021.07.002.

Ward, M., Tulloch, A.I.T., Radford, J.Q., Williams, B.A., Reside, A.E., Macdonald, S.L., Mayfield, H.J., Maron, M., Possingham, H.P., Vine, S.J., O'Connor, J.L., Massingham, E.J., Greenville, A.C., Woinarski, J.C.Z., Garnett, S.T., Lintermans, M., Scheele, B.C., Carwardine, J., Nimmo, D.G., Lindenmayer, D.B., Kooyman, R.M., Simmonds, J.S., Sonter, L.J., and Watson, J.E.M., 2020, Impact of 2019–2020 mega-fires on Australian fauna habitat: Nature Ecology and Evolution, v. 4, p. 1321–1326.

Waschbusch, P., Korsch, R.J., and Beaumont, C., 2009, Geodynamic modelling of aspects of the Bowen, Gunnedah, Surat and Eromanga basins from the perspective of convergent margin processes: Australian Journal of Earth Sciences, v. 56, p. 309–334.

Watson, A., Lovelock, J.E., and Margulis, L., 1978, Methanogenesis, fires and the regulation of atmospheric oxygen: BioSystems, v. 10, p. 293–298.

Watson, A.J. and Lovelock, J.E., 2013, The dependence of flame spread and probability of ignition on atmospheric oxygen: an experimental investigation, *in* C.M. Belcher (ed.), Fire Phenomena and the Earth System: An Interdisciplinary Guide to Fire Science: Wiley-Blackwell, Oxford, p. 273–287.

Weaver, L., McLoughlin, S., and Drinnan, A.N., 1997, Fossil woods from the Upper Permian Bainmedart Coal Measures, northern Prince Charles Mountains, East Antarctica: AGSO Journal of Australian Geology and Geophysics, v. 16, p. 655–676.

Webb, J.A. and Fielding, C.R., 1993, Permo–Triassic sedimentation within the Lambert Graben, northern Prince Charles Mountains, Antarctica, *in* R.H. Finlay, R. Unrug, M.R. Banks, and J.J. Veevers (eds.), Gondwana Eight: AA Balkema, Rotterdam, p. 357–369.

Wheeler, A., Van de Wetering, N., Esterle, J.S., and Götz, A.E., 2020, Palaeoenvironmental changes recorded in the palynology and palynofacies of a Late Permian Marker Mudstone (Galilee Basin, Australia): Palaeoworld, v. 29, p. 439–452, doi: 10.1016/j.palwor.2018.10.005.

Whiteside, J.H. and Grice, K., 2016, Biomarker records associated with mass extinction events: Annual Review of Earth and Planetary Sciences, v. 44, p. 581–612.

Whitman, E., Parisien, M.-A., Thompson, D.K., and Flannigan, M.D., 2019, Short-interval wildfire and drought overwhelm boreal forest resilience: Scientific Reports, v. 9, article 18796, doi: 10.1038/s41598-019-55036-7.

Wieting, C., Ebel, B.A., and Singha, K., 2017, Quantifying the effects of wildfire on changes in soil properties by surface burning of soils from the Boulder Creek Critical Zone Observatory: Journal of Hydrology: Regional Studies, v. 13, p. 43–57, doi: 10.1016/j.ejrh.2017.07.006.

Wignall, P.B., 2001, Large igneous provinces and mass extinctions: Earth-Science Reviews, v. 53, p. 1–33.

Wildman, R.A., Hickey, L.J., Dickinson, M.B., Berner, R.A., Robinson, J.M., Dietrich, M., Essenhigh, R.H., and Wildman, C.B., 2004, Burning of forest materials under late Paleozoic high atmospheric oxygen levels: Geology, v. 32, p. 457–460, doi: 10.1130/G20255.1.

Williams, P.R., 2000, Fire-stimulated rainforest seedling recruitment and vegetative regeneration in a densely grassed wet sclerophyll forest of north-eastern Australia: Australian Journal of Botany, v. 48, p. 651–658, doi: 10.1071/BT99020.

Wu, J., Baartman, J.E.M., and Nunes, J.P., 2020, Comparing the impacts of wildfire and meteorological variability on hydrological and erosion responses in a Mediterranean catchment: Land Degradation and Development, v. 32, p. 640–653, doi: 10.1002/ldr.3732.

Wu, Y., Chu, D., Tong, J., Song, H., Dal Corso, J., Wignall, P.B., Song, H., Du, Y., and Cui, Y., 2021, Six-fold increase of atmospheric pCO_2 during the Permian–Triassic mass extinction: Nature Communications, v. 12, article 2137.

Xiao, L., Zhao, Q., Wang, J., Mishra, V., Arbuzov, S.I., and Zhang, M., 2020, Wildfire evidence from the Middle and Late Permian Hanxing Coalfield, North China Basin: Geologica Acta, v. 18, p. 1–11.

Yan, Z.M., Shao, L.Y., Glasspool, I.J., Wang, J., Wang, X.T., and Wang, H., 2019, Frequent and intense fires in the final coals of the Paleozoic indicate elevated atmospheric oxygen levels at the onset of the end-Permian Mass Extinction Event: International Journal of Coal Geology, v. 207, p. 75–83.

Zhang, H., Cao, C.-q., Liu, X.-l., Mu, L., Zheng, Q.-f., Liu, F., Xiang, L., Liu, L.-j., and Shen, S.-z., 2016, The terrestrial end-Permian mass extinction in South China: Palaeogeography, Palaeoclimatology, Palaeoecology, v. 448, p. 108–124.

Zhou, W., Algeo, T.J., Luo, G., Xiaoyan, R., Chen, Z.-Q., and Xie, S., 2021, Hydrocarbon compound evidence in marine successions of South China for frequent wildfires during the Permian–Triassic transition: Global and Planetary Change, v. 200, article 103472, doi: 10.1016/j.gloplacha.2021.103472.

Received 17 October 2021; accepted 14 March 2022.